Published OnlineFirst May 31, 2016; DOI: 10.1158/2159-8290.CD-15-1177

RESEARCH ARTICLE

Obesity-Induced Inflammation and Desmoplasia Promote Pancreatic Cancer Progression and Resistance to Chemotherapy AC

Joao Incio[1,2,3], Hao Liu[1,4], Priya Suboj[1,5], Shan M. Chin[1], Ivy X. Chen[1,6], Matthias Pinter[1], Mei R. Ng[1], Hadi T. Nia[1], Jelena Grahovac[1], Shannon Kao[1], Suboj Babykutty[1,7], Yuhui Huang[1], Keehoon Jung[1], Nuh N. Rahbari[1], Xiaoxing Han[1], Vikash P. Chauhan[1], John D. Martin[1], Julia Kahn[1], Peigen Huang[1], Vikram Desphande[8], James Michaelson[8,9], Theodoros P. Michelakos[10], Cristina R. Ferrone[8,10], Raquel Soares[3], Yves Boucher[1], Dai Fukumura[1], and Rakesh K. Jain[1]

Published OnlineFirst May 31, 2016; DOI: 10.1158/2159-8290.CD-15-1177

ABSTRACT It remains unclear how obesity worsens treatment outcomes in patients with pancreatic ductal adenocarcinoma (PDAC). In normal pancreas, obesity promotes inflammation and fibrosis. We found in mouse models of PDAC that obesity also promotes desmoplasia associated with accelerated tumor growth and impaired delivery/efficacy of chemotherapeutics through reduced perfusion. Genetic and pharmacologic inhibition of angiotensin-II type-1 receptor reverses obesity-augmented desmoplasia and tumor growth and improves response to chemotherapy. Augmented activation of pancreatic stellate cells (PSC) in obesity is induced by tumor-associated neutrophils (TAN) recruited by adipocyte-secreted IL1β. PSCs further secrete IL1β, and inactivation of PSCs reduces IL1β expression and TAN recruitment. Furthermore, depletion of TANs, IL1β inhibition, or inactivation of PSCs prevents obesity-accelerated tumor growth. In patients with pancreatic cancer, we confirmed that obesity is associated with increased desmoplasia and reduced response to chemotherapy. We conclude that cross-talk between adipocytes, TANs, and PSCs exacerbates desmoplasia and promotes tumor progression in obesity.

SIGNIFICANCE: Considering the current obesity pandemic, unraveling the mechanisms underlying obesity-induced cancer progression is an urgent need. We found that the aggravation of desmoplasia is a key mechanism of obesity-promoted PDAC progression. Importantly, we discovered that clinically available antifibrotic/inflammatory agents can improve the treatment response of PDAC in obese hosts. *Cancer Discov; 6(8); 852–69. ©2016 AACR.*

See related commentary by Bronte and Tortora, p. 821.

INTRODUCTION

Pancreatic cancer is the fourth-leading cause of cancer-associated death worldwide, with an overall 5-year survival rate of 7% (1). The risk of pancreatic cancer is about 50% greater for individuals with obesity, particularly those with increased abdominal adiposity (2). Excess body weight also worsens the already dismal outcome of patients with pancreatic ductal adenocarcinoma (PDAC) by increasing the relative risk of cancer mortality by more than 2-fold (3–7). As a consequence of the obesity pandemic—with nearly 70% of the U.S. adult population being either overweight or obese (8)—the majority of patients with PDAC present with excess weight at diagnosis (6). Thus, understanding why obesity is associated with a worse prognosis might lead to novel treatments and enhance the outcome of current therapies.

PDAC is a highly desmoplastic cancer characterized by activated pancreatic stellate cells (PSC) and an excessive accumulation of extracellular matrix (ECM; refs. 9, 10). ECM components and PSCs directly promote the survival and migration of cancer cells (11–13). In addition, the interaction between cancer cells, stromal cells (e.g., PSCs), and the ECM produces physical forces (solid stress—pressure from solid tissue components) which compress tumor blood vessels, thus causing poor and heterogeneous tumor perfusion (14, 15). These mechanically induced changes in vascular perfusion create a formidable barrier to delivery and efficacy of chemotherapeutics, leading to poorer treatment outcomes (11, 16–19). Importantly, obesity itself is a prodesmoplastic condition. The hypoxia that results from abnormal blood vessels and decreased blood flow due to the rapidly expanding white adipose tissue (WAT) in obesity causes adipocyte dysfunction and immune cell recruitment (20–22). The latter leads to cytokine production, inflammation, and ultimately fibrosis (20–22). In particular, adipocytes in WAT abundantly express the angiotensin II type-1 receptor (AT1; refs. 23, 24), a major profibrotic pathway that becomes activated in a proinflammatory environment (23, 24). Obesity also leads to fat accumulation in the normal

[1]Edwin L. Steele Laboratories, Department of Radiation Oncology, Massachusetts General Hospital, Harvard Medical School, Boston, Massachusetts. [2]Department of Internal Medicine, Hospital S. Joao, Porto, Portugal. [3]I3S, Institute for Innovation and Research in Heath, Metabolism, Nutrition and Endocrinology Group, Biochemistry Department, Faculty of Medicine, Porto University, Porto, Portugal. [4]Biology and Biomedical Sciences, Harvard Medical School, Boston, Massachusetts. [5]Department of Botany and Biotechnology, St. Xaviers College, Thumba, Trivandrum, Kerala, India. [6]Harvard School of Engineering and Applied Sciences, Harvard University, Cambridge, Massachusetts. [7]Department of Zoology, Mar Ivanios College, Nalanchira, Trivandrum, Kerala, India. [8]Department of Pathology, Massachusetts General Hospital, Harvard Medical School, Boston, Massachusetts. [9]Laboratory for Quantitative Medicine, and Division of Surgical Oncology, Gillette Center for Women's Cancers, Massachusetts General Hospital and Harvard Medical School, Boston, Massachusetts. [10]Departments of Gastroenterology and Surgery, Massachusetts General Hospital, Harvard Medical School, Boston, Massachusetts.

Note: Supplementary data for this article are available at Cancer Discovery Online (http://cancerdiscovery.aacrjournals.org/).

Current address for Y. Huang: Cyrus Tang Hematology Center, Soochow University, Jiangsu, China; current address for N.N. Rahbari: Department of Surgery, Technical University Dresden, Dresden, Germany; current address for V.P. Chauhan: Koch Institute for Integrative Cancer Research, Massachusetts Institute of Technology, Cambridge, MA; and current address for J.D. Martin: Department of Bioengineering, Graduate School of Engineering, The University of Tokyo, Tokyo, Japan.

Corresponding Authors: Rakesh K. Jain, Massachusetts General Hospital, 100 Blossom Street, Cox 7, Boston, MA 02114. Phone: 617-726-4083; Fax: 617-724-1819; E-mail: jain@steele.mgh.harvard.edu; and Dai Fukumura, Phone: 617-726-8143; Fax: 617-724-5841; E-mail: dai@steele.mgh.harvard.edu

doi: 10.1158/2159-8290.CD-15-1177

Published OnlineFirst May 31, 2016; DOI: 10.1158/2159-8290.CD-15-1177

pancreas (steatosis), which generates a similar inflammatory process within the pancreas itself, with increased expression of cytokines, ECM remodeling, and fibrosis (7, 25, 26). Importantly, cancer lesions in obese mice and patients have an increased adipocyte content (27, 28). Of clinical relevance, the interaction of cancer cells with adipocytes—both in the form of accumulation of fat in the pancreas and at the invasive tumor front into the local adipose tissue—is associated with worse outcomes in patients with PDAC (7, 29). However, the role of adipocytes during obesity-induced PDAC progression remains unclear.

We have previously reported that obesity promotes inflammation (increased IL1β levels) and immune cell infiltration in PDACs, which associates with increased tumor growth and metastasis (30). Here, we hypothesized that the obesity-associated adipocyte accumulation in PDACs generates a proinflammatory and profibrotic microenvironment, which promotes tumor progression, and hinders the delivery and efficacy of chemotherapy. In this study, we tested this hypothesis in patients with pancreatic cancer as well as in clinically relevant orthotopic and genetically engineered mouse models of PDAC. To reduce the obesity-instigated desmoplastic reaction in PDAC, we used AT1 knockout (*Agtr1a*$^{-/-}$) mice and the FDA-approved AT1 blocker (ARB) losartan, which as we previously demonstrated reduces PSC activation, desmoplasia, and solid stress in PDAC (18). In addition, we examined whether the obesity-exacerbated desmoplasia in PDAC results from increased inflammation and immune cell infiltration, and we uncovered the cellular and molecular mechanisms involved.

RESULTS

Diet-Induced or Genetically Induced Obesity Promotes Pancreatic Tumor Progression

We fed a high-fat diet (HFD) to four different strains of mice to generate diet-induced obesity (DIO; Fig. 1A). In addition, we used a genetic model of leptin deficiency (*ob/ob*; Fig. 1A). Consistent with previous studies including those from our laboratory (27, 30, 31), obesity promoted tumor initiation and progression across various tumor models. Using spontaneous PDAC models—KPC (*Ptf1-Cre/Kras*$^{LSL\text{-}G12D/+}$*/Trp53*$^{LSL\text{-}R172H/+}$) and iKRAS (*Ptf1-Cre/ROSA26-LSL-rtTa-IRES-eGFP/TetO-Kras*$^{TetO\text{-}LSL\text{-}G12D}$*/Trp53*$^{L/+}$) mice (32–35)—we found that obese animals tended to develop tumors earlier than lean mice (Supplementary Fig. S1). Furthermore, DIO and genetically induced obesity accelerated the growth of implanted tumors in two orthotopic syngeneic PDAC models—PAN02 and AK4.4. Similar to our previous observations (30), in comparison with lean mice, obese mice presented with increased tumor weight (Fig. 1B), increased metastatic dissemination to the mesenteric peritoneum in the PAN02 model (Fig. 1Ci and ii), and increased

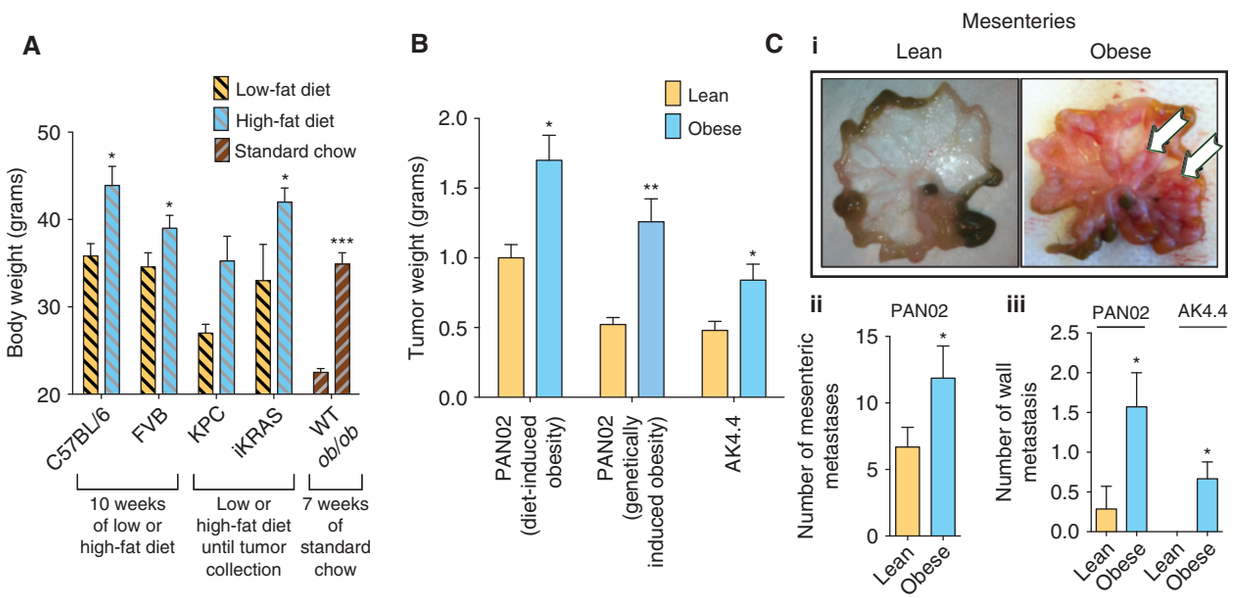

Figure 1. Obesity promotes tumor initiation and progression. **A,** generation of obese mouse models. High-fat (60%) versus low-fat (10%) diets started at 6 weeks of age generated a difference in body weight in multiple models. Data represent the body weight of WT C57BL/6 and FVB mice after 10 weeks on diet, and of the spontaneous PDAC models (KPC and iKRAS) at the time of tumor collection (between 15 and 20 weeks of diet for KPC, 12 to 16 weeks for iKRAS). Body weight of mice genetically deficient for leptin (*ob/ob*) or age-matched WT mice was recorded after 7 weeks on a standard chow ($n = 8$–10/group for C57BL/6, FVB, and *ob/ob*; 4–10/group for KPC; 7–21/group for iKRAS). **B,** effect of obesity on tumor growth. Data in this panel represent the weight of tumors collected 3 weeks after implantation. PAN02 and AK4.4 syngeneic tumors were orthotopically implanted in C57BL/6 and FVB mice, respectively, at 10 weeks of diet (diets were continued until tumor collection); *ob/ob* mice and corresponding age-matched WT mice were implanted with PAN02 tumors at 7 weeks of age (mice under standard chow). Obese animals presented with higher tumor weights than lean counterparts in all models ($n = 8$–10/group). **C,** effect of obesity on metastasis. **Ci,** representative images of mesenteric peritoneal dissemination observed in lean and obese mice 3 weeks after implantation of PAN02 tumors. White arrows, metastatic nodules in the mesentery. **Cii,** quantification of mesenteric peritoneal metastasis in the PAN02 model ($n = 26$–30/group). **Ciii,** quantification of retroperitoneal metastasis in the PAN02 model and AK4.4 model ($n = 4$–7/group). Data are shown as mean ± SEM. *P* values were determined by the Student *t* test. *, $P < 0.05$; **, $P < 0.01$; ***, $P < 0.001$.

Published OnlineFirst May 31, 2016; DOI: 10.1158/2159-8290.CD-15-1177

local invasion into the retroperitoneum in both models (Fig. 1Ciii). Taken together, the mouse models used confirmed the tumor-promoting effect of obesity in PDAC.

Obesity Induces a Steatotic and Fibrotic Microenvironment in PDACs

The dysfunctional hypertrophic adipocytes that accumulate in visceral adipose and pancreatic tissues in obesity lead to the development of a local desmoplastic reaction characterized by fibrosis and inflammation (20–22). In tumors, desmoplasia promotes tumor growth and impairs response to chemotherapy via reduced vessel perfusion (18). We hypothesized that obesity augments desmoplasia in the pancreatic tumor microenvironment, thus stimulating tumor progression. As expected (24), in obese mice we observed hypertrophic adipocytes and associated fibrosis in the visceral adipose tissue (Fig. 2Ai). Importantly, we found that the tumor microenvironment also contained more and larger adipocytes (Fig. 2Ai and iii). In part, this was due to tumors invading the neighboring visceral WAT (Supplementary Fig. S2A and S2B), as reported in patients with pancreatic cancer (7, 29). Furthermore, Masson's trichrome staining revealed an abundant fibrosis in tumor areas enriched in adipocytes or alongside adjacent visceral adipose tissues (Fig. 2Ai and iv; Supplementary Figs. S2C and S3A). These data suggest that, in obesity, PDACs adopt a fibrotic adipose microenvironment as they invade the adjacent fibrotic adipose tissues. We next determined whether the abundance of fibrotic adipocyte-rich areas in tumors from obese mice led to an overall increase in tumor fibrosis. Using second harmonic generation (SHG) imaging, we found that obesity significantly increased the SHG signal, which represents fibrillar collagen, in orthotopically grown PAN02 and AK4 tumors (Fig. 2Bi and iii). Obesity also significantly increased collagen-I expression (immunofluorescence) in the lesions of orthotopic and spontaneous PDACs (Fig. 2Bii and iv). Of note, within each body-weight setting, collagen-I levels did not correlate with tumor area, indicating that tumor size alone (increased in obesity) is not responsible for the observed increase in fibrosis in obese mice (Supplementary Fig. S3B). The tumor levels of hyaluronan (HA)—an ECM molecule also associated with desmoplasia—also tended to be higher in obese mice (Supplementary Fig. S3C and S3D). We then determined whether the presence of activated PSCs was also increased in tumors in obese mice. In obese animals, immunofluorescence staining revealed a significant increase in the density of alpha-smooth muscle actin (αSMA)–positive PSCs in PAN02 (Fig. 2Ci and ii). The numbers of αSMA-positive PSCs in AK4.4 and KPC models also tended to be higher in obese mice, and immunoblotting confirmed significant increases of αSMA in PAN02 and AK4.4 tumors (Fig. 2Ci and ii; Supplementary Fig. S3E; see also

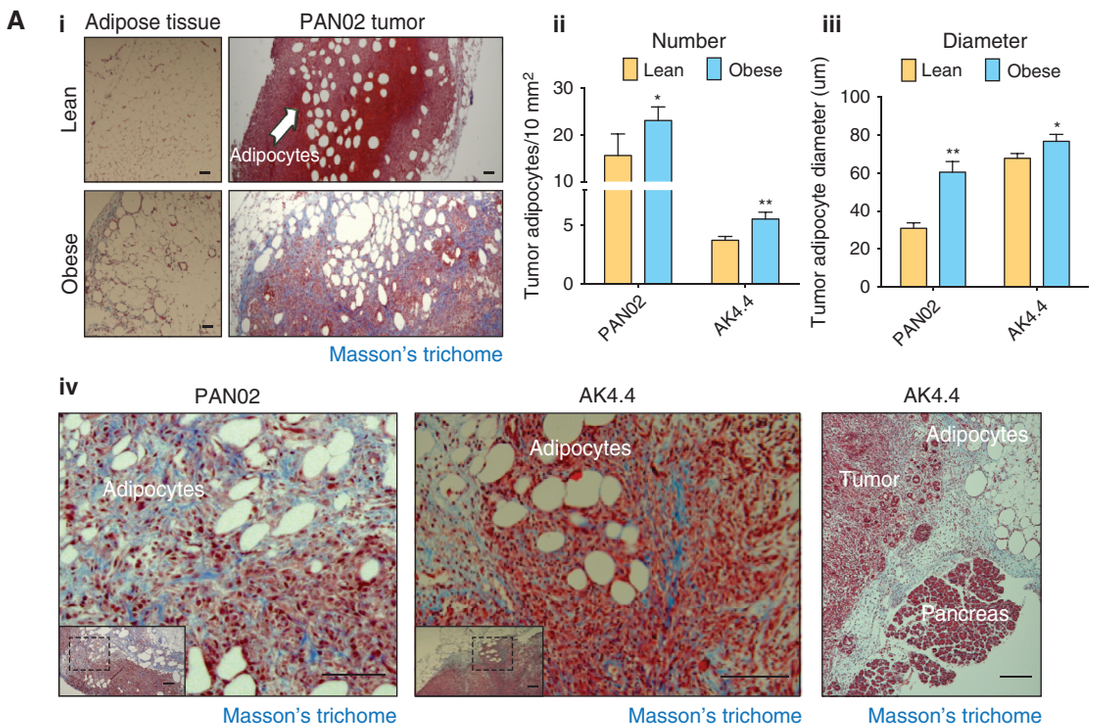

Figure 2. Obesity aggravates tumor desmoplasia. **A,** description of the adipose microenvironment in tumors from obese mice. **Ai,** adipocyte enlargement and fibrosis in visceral adipose tissue and tumors from obese mice. Masson's trichrome staining denotes fibrosis in blue. Arrows, adipocytes; scale bars, 200 μm. Adipocyte count (**Aii**) and size (**Aiii**) in PAN02 and AK4.4 tumors, indicating an enrichment of enlarged adipocytes in the tumor microenvironment in obese mice [$n = 3$ tumors/group, 8 regions of interest (ROI)/tumor]. **Aiv,** representative images of the adipose tissue–tumor interaction, revealing increased expression of fibrosis where tumors invade the adjacent adipose tissue. On the left and center, enlarged images of dashed area in the left bottom inset are shown. On the right, tumor epithelium is observed in close proximity to fibrotic adipose tissue and normal pancreas. Tumor sections were stained for Masson's trichrome. Scale bars, 100 μm (PAN02), 200 μm (AK4.4, center), 500 μm (AK4.4, right). (*continued on next page*)

Published OnlineFirst May 31, 2016; DOI: 10.1158/2159-8290.CD-15-1177

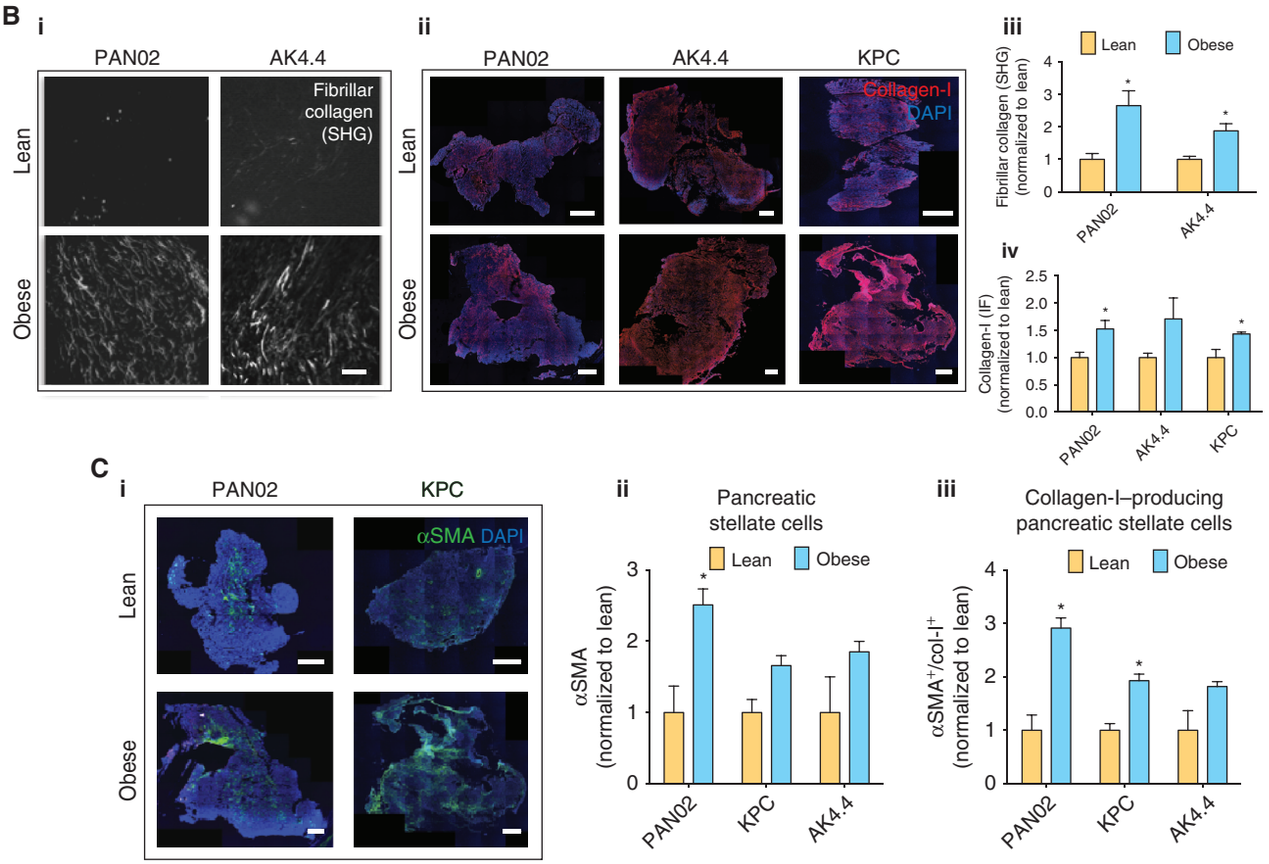

Figure 2. ***(Continued)*** **B,** collagen levels in PDACs. **Bi,** representative pictures of fibrillar collagen in tumors using SHG. Scale bar, 100 μm. **Bii,** representative pictures of collagen-I staining [immunofluorescence (IF)] in tumors. Scale bars, 1 mm. **Biii,** quantification of fibrillar collagen normalized to lean animals. Tumors from obese mice presented with increased expression of fibrillar collagen in PAN02 and AK4.4 orthotopic PDACs. **Biv,** quantification of collagen expression normalized to lean animals. Tumors from obese mice presented with increased collagen-I expression in three different tumor models ($n = 3$–6/group). **C,** effect of obesity on αSMA expression in PDACs. **Ci,** representative pictures of αSMA expression in AK4.4, PAN02, and KPC tumors by immunofluorescence. Scale bars, 1 mm. **Cii,** quantification of αSMA expression by immunofluorescence was performed as a percentage of αSMA (**Cii**), as well as a percentage of double-positive αSMA/col-I expression normalized to lean animals (**Ciii**; $n = 3$–6/group). For representative pictures of αSMA/col-I double staining in PAN02 and AK4.4 tumors, please see Supplementary Fig. S3C and S3D. Data are shown as mean ± SEM. *P* values were determined by the Student *t* test. *, $P < 0.05$; **, $P < 0.01$.

Fig. 4C). We confirmed that αSMA-expressing PSCs associate with collagen-I expression in our PDAC models (Supplementary Fig. S3F and S3G). Importantly, the percentage of PSCs associated with collagen-I expression increased by 2- to 3-fold in the obese setting (Fig. 2Ciii). Consistent with the increase in the fibrotic reaction in adipocyte-rich regions in tumors, the expression of αSMA also increased in these regions (Fig. 6Bi and ii). Taken together, we found that tumors in the obese setting are enriched in enlarged adipocytes, activated PSCs, and collagen-I.

Obesity-Aggravated Desmoplasia Is Associated with Impaired Vascular Perfusion, Intratumoral Drug Delivery, and Treatment Efficacy

We have reported that desmoplasia reduces the delivery and efficacy of chemotherapy in PDAC by decreasing vessel perfusion (18). Therefore, we tested if obesity-augmented desmoplasia reduced the efficacy of chemotherapy. Indeed, we found that in obese animals, the tumor vascular perfusion was reduced (Fig. 3Ai–iii). In both PAN02 and AK4.4 tumors, the percentage of perfused vessels per total tumor area significantly decreased from 2.5% to 0.75% (from ~25% to 10% of total vessel area). Consistent with this finding, we observed an increase in hypoxia markers in tumors from obese mice (Fig. 3B; Supplementary Fig. S4). To determine if reduced perfusion impairs the delivery of chemotherapeutic agents, we measured the uptake of 5-Fluorouracil (5-FU), an approved cytotoxic agent used in the treatment of PDAC (36). Obesity significantly decreased the uptake of 5-FU in PAN02 tumors (Fig. 3C) and reduced the efficacy of 5-FU chemotherapy in both PAN02 and AK4.4 tumors (Fig. 3D). The 5-FU treatment significantly reduced the tumor weight in lean mice (Fig. 3D). In contrast, in obese mice, 5-FU did not significantly affect the growth of PAN02 and AK4.4 tumors (Fig. 3D). Collectively, these data show that, in addition to directly promoting PDAC growth and metastasis, obesity reduces vascular perfusion, drug delivery, and the efficacy of 5-FU chemotherapy.

Published OnlineFirst May 31, 2016; DOI: 10.1158/2159-8290.CD-15-1177

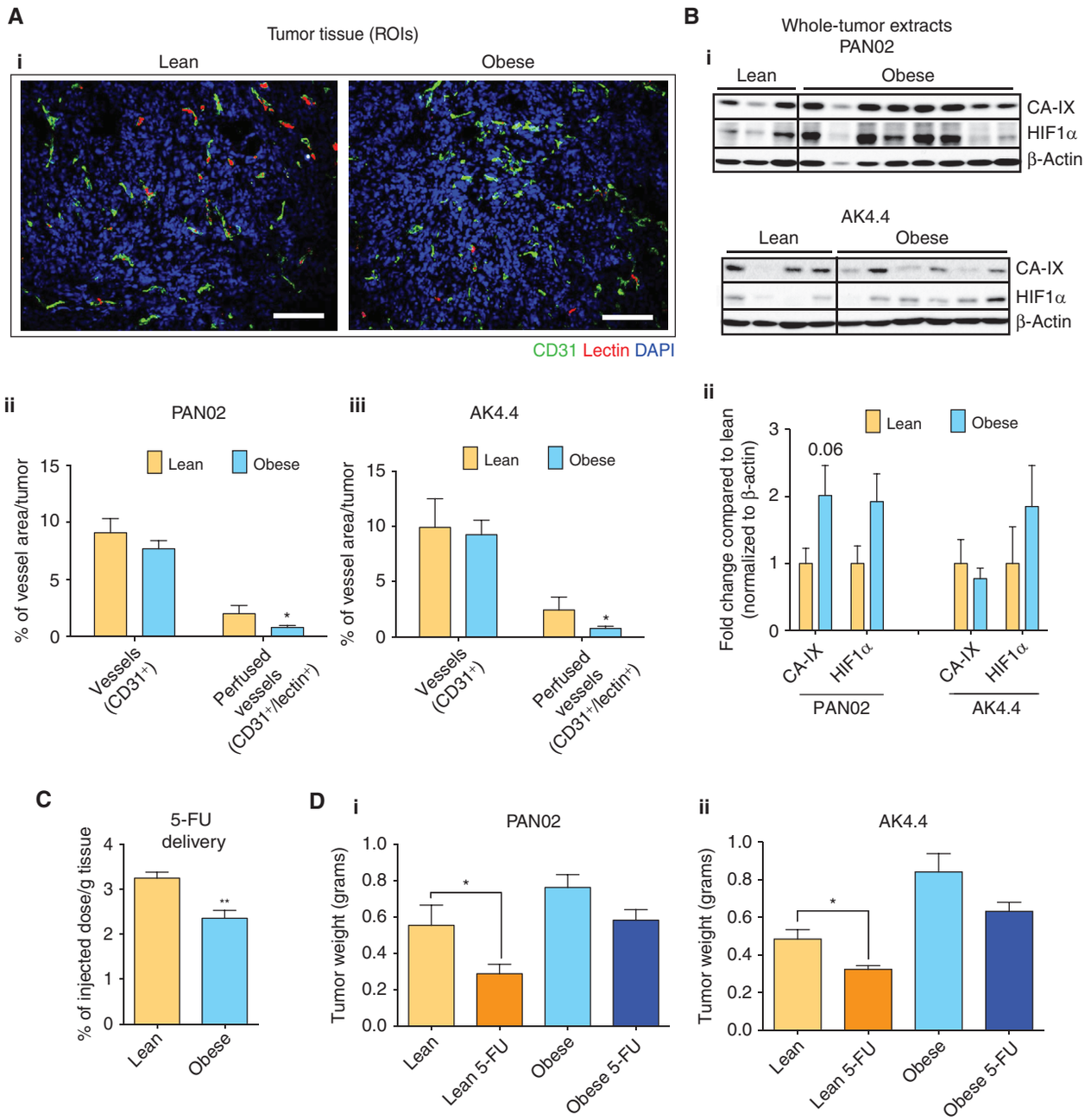

Figure 3. Obesity-aggravated desmoplasia is associated with impaired perfusion, oxygenation, drug delivery, and resistance to chemotherapy. **A,** effect of DIO on tumor perfusion. **Ai,** representative pictures of CD31⁺ vessels and lectin in PAN02 tumors. Scale bars, 200 μm. **Aii–iii,** quantification of total (CD31⁺) and lectin-positive (CD31/lectin⁺) vessel area in PAN02 (**ii**) and AK4.4 (**iii**) tumors. Obese mice presented with decreased perfusion ($n = 3$–12 tumors/group). **B,** effect of DIO on tumor hypoxia. **Bi,** each lane represents the protein expression of hypoxia markers in individual PAN02 or AK4.4 tumors. **Bii,** densitometric analysis (fold change compared with the lean group) normalized to β-actin ($n = 4$–15, see additional bands in Supplementary Fig. S4). Obese mice presented with increased hypoxia in tumors. **C,** effect of DIO on the delivery of chemotherapy to PAN02 tumors. 5-FU quantified via high-performance liquid chromatography (HPLC). Obesity decreased delivery of the chemotherapeutic agent ($n = 4$ tumors/group). **D,** Effect of DIO on response to chemotherapy. PAN02 and AK4.4 tumors were orthotopically implanted at 10 weeks of diet, treatments were initiated at day seven after implantation, and tumors were resected at day 19 (after three cycles of 5-FU 30 mg/kg q4d). 5-FU was less effective in preventing tumor growth in obese animals than in lean (two-way ANOVA, $n = 6$–10/group). Data are shown as mean ± SEM. *P* values were determined by the Student *t* test unless otherwise stated. *, $P < 0.05$; **, $P < 0.01$.

Published OnlineFirst May 31, 2016; DOI: 10.1158/2159-8290.CD-15-1177

The Inhibition of AT1 Signaling Reduces Obesity-Induced Desmoplasia and Tumor Growth and Increases the Response to Chemotherapy

We have shown that tumor desmoplasia results in part from the activation of PSCs through AT1 signaling (18). We confirmed the expression of AT1 in PSCs (AT1/αSMA double staining), which ranged from 70.3% (SEM = 5.7) in PSCs in PAN02 tumors to 35.3% (SEM = 12.8) in AK4.4 tumors (Supplementary Fig. S5A). We next analyzed the effects of obesity on AT1 downstream pathways. In both PAN02 and AK4.4 tumors, obesity increased the activation of p38, ERK, AKT, and their targets pS6 and 4EBP1 (Fig. 4A; refs. 18, 37–39). In addition, several target genes of the AT1 pathway, including *Col1a2*, *Tgfβ1*, and matrix metalloproteinases genes, were upregulated (Fig. 4Bi and ii; Supplementary Tables S1–S2).

To test if the inhibition of AT1 signaling could reverse desmoplasia in obese mice, we used the ARB losartan and mice deficient in AT1 (*Agtr1a*$^{-/-}$). In AK4.4 tumors in obese but not lean mice, the 16-day losartan treatment significantly reduced the gene and protein expression of the PSC-activation marker αSMA (Fig. 4Ci and ii; Supplementary Fig. S5B). Similarly, in obese mice, losartan significantly decreased the SHG signal for fibrillar collagen and reduced collagen-I immunofluorescence, though not significantly (Fig. 4Di–iv). Moreover, in AK4.4, losartan normalized the obesity-induced expression of desmoplasia-related markers (αSMA, decorin, SMAD2, p-p38) and ECM remodeling (MMP9; Fig. 4Ei and ii; and Supplementary Fig. S5B). These effects were absent or only modest in lean animals, consistent with the small reduction in αSMA expression in this weight setting. Similarly, in obese mice with PAN02 tumors, losartan significantly reduced the collagen-I content (Fig. 4Dv), and losartan or AT1 deletion reduced the expression of αSMA (Supplementary Fig. S3Ei and S3Eii; Supplementary Fig. S5C). Furthermore, intimately associated with AT1 signaling, the epithelial-to-mesenchymal (EMT) markers MMP9, SNAIL, and vimentin were increased in AK4.4 tumors from obese mice in both models and were subsequently normalized by losartan (Fig. 4E; Supplementary Fig. S5B). In PAN02 tumors, we confirmed that AT1 deletion normalized the obesity-increased expression of vimentin (Supplementary Fig. S3Ei and S3Eiii).

We then determined whether AT1 blockade could improve the response to chemotherapy, particularly in obese mice with desmoplastic tumors. In a previous study, we found that losartan combined with 5-FU significantly inhibited the growth of AK4.4 tumors in mice fed a regular diet, but losartan alone had no effect on tumor growth (18). Consistent with this, in the current study in lean mice, the genetic deletion of AT1 or the losartan treatment had no effect on tumor size in PAN02 and AK4.4 models. However, in obese mice with a genetic deletion of AT1 or treated with losartan, the tumor sizes were significantly smaller (Fig. 4Fi and ii). Similar to the data of Fig. 3D, 5-FU alone significantly reduced the size of AK4.4 and PAN02 tumors in lean but not in obese mice. The combination of genetic AT1 blockade plus 5-FU significantly reduced tumor size compared with either treatment alone in obese but not in lean animals (Fig. 4Fi). Similarly, in both AK4.4 and PAN02 tumors, losartan significantly enhanced the response to 5-FU in obese but not in lean animals, although it was still somewhat effective in the lean setting in the AK4.4 model (Fig. 4Fi and ii). However, because losartan alone was effective in decreasing tumor growth in obese mice (Fig. 4Fi and ii; Supplementary Fig. S5D), the tumor size in losartan- versus losartan plus 5-FU–treated groups in obese mice did not significantly differ (Fig. 4Fi and ii). Importantly, we confirmed via abdominal ultrasound that, when treatment was initiated, tumors had similar size in all groups (lean and obese, control vs. losartan; Supplementary Fig. S5D). In addition to AT1, we recently observed that PSCs also express the angiotensin II type-2 receptor (AT2), which has antifibrotic effects as opposed to the profibrotic effects of AT1 signaling (18). However, we found here that the PAN02 tumor response to chemotherapy in *AT2*$^{-/-}$ mice was similar to that in wild-type (WT) mice, regardless of diet group (Fig. 4Fi).

Similar to our previous study (18), we analyzed whether the increase in 5-FU antitumor efficacy induced by losartan in obese animals could be at least in part due to improvements in vascular perfusion and drug delivery. In both AK4.4 and PAN02 models, we found a trend for increased tumor

Figure 4. Blockade of AT1 reverses the obesity-aggravated desmoplasia and improves response to chemotherapy. **A,** effect of obesity on activation of major signaling pathways in tumors. **Ai,** each lane represents the protein expression in individual tumors. **Aii,** densitometric analysis normalized to β-actin. Obesity associates with increased signaling activity. **B,** effect of obesity on target genes of AT1 signaling. Depicted genes where at least an approximately 2-fold change in mRNA expression was observed in either tumor model. Data normalized to lean group. Three to 4 samples per group pooled in one single PCR array fibrosis gene set plate. Expression of genes associated with AT1 pathway activation and fibrosis/desmoplasia is increased in PAN02 and AK4.4 tumors from obese mice. **C,** effect of losartan (los) on αSMA expression in AK4.4 tumors. **Ci,** each lane represents the protein expression in individual tumors. Losartan reduced tumor αSMA protein expression more dramatically in the obese setting. **Cii,** densitometric analysis normalized to tubulin. **D,** effect of losartan on collagen levels. Losartan reduced tumor fibrillar collagen as determined by SHG (**Di**) as well as collagen-I (Col-I) expression (**Dii**) in AK4.4 tumors from obese mice. Scale bars, 100 μm (SHG) and 1 mm (Col-I). **Diii–v,** quantification of collagen was performed as a percentage of a region of interest (ROI) for SHG ($n = 4$ tumors/group, 8 ROIs per tumor) and as a percentage of viable tumor area in the whole tumor for collagen-I immunofluorescence ($n = 4$–6 tumors/group). **E,** effect of losartan on tumor desmoplasia and AT1 signaling–related markers in AK4.4 tumors from lean and obese mice. **Ei,** protein expression by Western blotting of AK4.4 tumors (each lane represents the protein expression in individual tumors) revealed that losartan normalized the obesity-augmented expression of several AT1 signaling and desmoplasia-related markers, i.e., AT1, TGFB, SMAD2, vimentin, SNAIL, MMP9, and phospho-p38. Of note, similar to αSMA, the changes in AT1, as well as other desmoplasia-related markers, were relatively mild in the lean setting. **Eii,** densitometric analysis normalized to tubulin (depicted are significant differences between control and losartan treatment). **F,** effect of pharmacologic and genetic blockade of AT1 on the efficacy of chemotherapy in the lean and obese setting. **Fi,** in the PAN02 model, losartan and AT1 genetic deficiency (*Agtr1a*$^{-/-}$ mice) improved response to chemotherapy in obese but not in lean animals. **Fii,** in the AK4.4 model, losartan improved response to chemotherapy in both lean and obese settings but with a higher magnitude in obese setting (**i** and **ii:** two-way ANOVA, $n = 4$–8 tumors/group. Depicted are significant differences between treatment groups compared with control or 5-FU groups). Note: For simplicity, not all significant differences are depicted. Data are shown as mean ± SEM with the exception of plots **Ai–ii**. *P* values were determined by the Student *t* test unless otherwise stated. *, $P < 0.05$; **, $P < 0.01$; *** $P < 0.001$.

Published OnlineFirst May 31, 2016; DOI: 10.1158/2159-8290.CD-15-1177

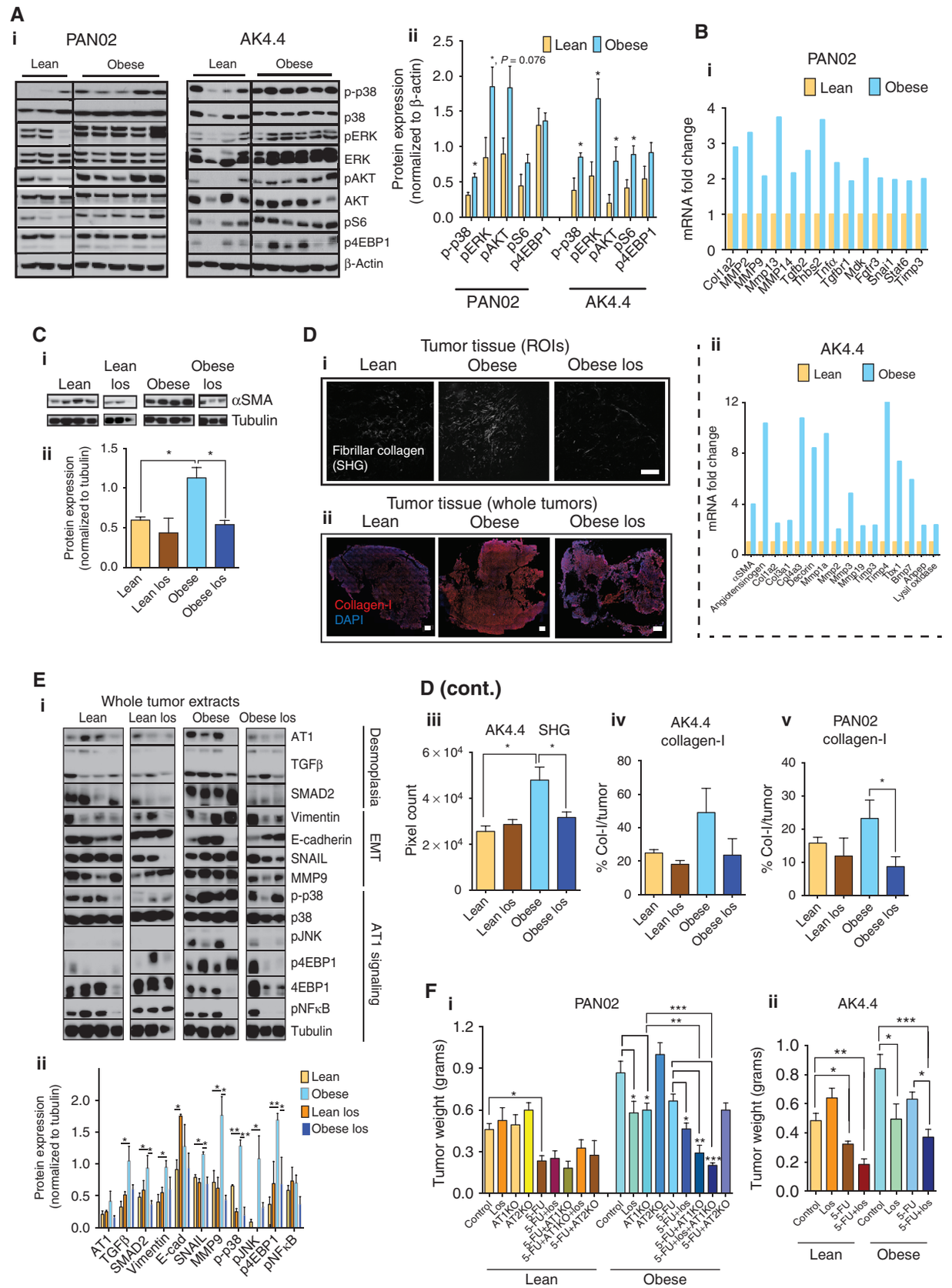

Published OnlineFirst May 31, 2016; DOI: 10.1158/2159-8290.CD-15-1177

perfusion and increased delivery of chemotherapeutics by AT1 blockade (Supplementary Fig. S5E and S5F). The mild effects on tumor perfusion could be the consequence of a reduced mean arterial blood pressure (MABP) induced by the relatively high dose of losartan (90 mg/kg/day). In fact, losartan reduced the MABP by approximately 27% in both lean and obese mice (Supplementary Fig. S5G). Of note, AT1 blockade did not induce greater loss in body weight in tumor-bearing mice compared with WT, suggesting that based on this parameter, it does not appear to cause overall toxicity (Supplementary Fig. S5H).

In conclusion, we found that obesity is associated with increased AT1 signaling in tumors; that in obese animals, losartan alone or the genetic blockade of AT1 has direct anti-tumor effects; and that AT1 inhibition can also enhance the efficacy of 5-FU chemotherapy.

Tumor-Associated Neutrophils Mediate Obesity-Induced PSC Activation and Tumor Progression

The fibrotic phenotype in adipose tissues and normal pancreas in obesity is largely the consequence of a persistent proinflammatory state, which is characterized by the production of cytokines by hypoxic and dysfunctional hypertrophic adipocytes and the recruitment of immune cells (21, 22, 34). In addition, we have previously described increased inflammation and immune cell recruitment in PAN02 tumors implanted in obese mice (30). Hence, we next determined here whether adipocyte-associated inflammation was responsible for the increased tumor desmoplasia and accelerated tumor growth observed in obese animals. Flow cytometric analysis revealed that obesity promotes the infiltration of $CD11b^+Gr1^+F4/80^-$ myeloid cells in orthotopic AK4.4 and PAN02 PDAC models in obese mice (Fig. 5A; Supplementary Fig. S6A). We subsequently confirmed that the majority of infiltrated myeloid cells were $Ly6G^+$ tumor-associated neutrophils (TAN; Supplementary Fig. S6B). In both PAN02 and AK4.4 tumors, TAN depletion (TAN-D)—with an anti-Ly6G antibody that decreased TAN infiltration by 90% (Supplementary Fig. S7A)—reverted the increased tumor growth in obese mice to levels in lean mice (Fig. 5Bi and ii). This effect occurred only when TAN-D was initiated on day 1 but not on day 7 of the experiment, indicating the relative importance of TANs in tumor progression at an early stage (Fig. 5Bi). In addition to a direct effect on tumor growth, we determined whether TANs could affect desmoplasia. We observed the preferential accumulation of TANs in areas with activated PSCs (Fig. 5C), suggesting a potential paracrine cross-talk between TANs and PSCs. Indeed, TAN-D in PAN02 tumors in obese animals decreased PSCs and the number of activated PSCs associated with collagen-I to levels in lean animals (Fig. 5Di and ii, and E). Consistent with this, we observed a significant reduction in AT1 expression and a trend for decreased collagen-I and MMP9 expression in PAN02 tumors (Fig. 5E). In addition, TAN-D significantly increased the vascular surface area and the number of perfused vessels in PAN02 tumors, but not significantly in AK4.4 tumors (Fig. 5F; Supplementary Fig. S7Bi and S7Bii). Our data suggest that obesity increases TAN recruitment in PDAC, which mediates the activation of PSCs and tumor growth.

IL1β Mediates Obesity-Induced TAN Infiltration and PSC Activation in PDACs

The obesity-induced proinflammatory/profibrotic response and immune cell recruitment that occur in adipose tissue are mediated by cytokine/chemokine production from dysfunctional adipocytes, such as IL1β and IL6 (21, 22, 40). Hence, we determined whether these inflammatory cytokines mediated obesity-induced fibrotic processes and TAN infiltration in the tumor microenvironment. We confirmed our previous observation (30) that in PAN02, obesity significantly increased the expression of IL1β by 5-fold and induced a trend toward increased expression of IL6, TNFα, IL12, or CXCL1 (Fig. 6A). Obesity also increased the levels of IL1β in AK4.4 tumors (Supplementary Fig. S8). Not surprisingly, IL1β was abundantly expressed by adipocytes in adipocyte-rich areas where activated PSCs predominate (Fig. 6Bi, top row figure, and ii). Antibody neutralization of IL1β (MM425B; Endogen/Pierce Biotechnology; 2 mg/Kg i.p. q4d)—in obese mice implanted with PAN02 tumors—significantly decreased TAN infiltration. In addition, the decreased TAN recruitment was associated with an increase in $CD8^+$ cytotoxic T-cell population (decreased in obese mice compared with lean) and a decrease in regulatory T cells (Treg; Fig. 6Ci and ii). Similar to TAN-D effects, IL1β inhibition in obese animals significantly reduced the growth of PAN02 tumors (Fig. 6D) as well as the expression levels of αSMA (Supplementary Fig. S3E). In addition, the EMT marker vimentin was also reduced by IL1β inhibition in obese mice (Supplementary Fig. S3E). In addition to adipocytes, IL1β was also expressed in about 70% of TANs themselves (Fig. 6E), and TAN-D reduced tumor IL1β levels (Fig. 6F). This suggests the presence of an autocrine mechanism that enables further TAN recruitment and potentiates inflammation and fibrosis. Furthermore, TAN-D significantly reduced the levels of CXCL1, indicating that this cytokine may also play a role in obesity-induced inflammation (Supplementary Fig. S9). In conclusion, our findings suggest IL1β is involved in obesity-induced TAN recruitment, immunosuppressive microenvironment, and PDAC progression.

AT1 Blockade Can Reciprocally Inhibit Inflammation and Immune Cell Infiltration in Obesity

We observed that αSMA-positive PSCs also abundantly (~70% of PSCs) expressed IL1β (Fig. 6Bii and G) and that of the total cells expressing IL1β, PSCs correspond to 40% of these cells in adipocyte-poor but 70% in adipocyte-rich (~70% increase) regions (Fig. 6Bi and ii). Because IL1β recruits TANs, which localize in close proximity to PSCs as shown above, we next examined whether targeting PSCs could also interfere with IL1β production and TAN recruitment, particularly in obese mice. Indeed, in obese mice, prevention of PSC activation by losartan inhibition of AT1 signaling decreased IL1β levels in AK4.4 and PAN02 tumors (Supplementary Fig. S10A). In addition, the genetic deletion of AT1 decreased TAN recruitment in PAN02 tumors in obese but not lean mice (Fig. 6Ci and ii). Consequently, recapitulating IL1β inhibition, AT1 blockade increased $CD8^+$ T cells and reduced Tregs in tumors from obese but not lean mice (Fig. 6Fi–iii). Similar trends were observed

Published OnlineFirst May 31, 2016; DOI: 10.1158/2159-8290.CD-15-1177

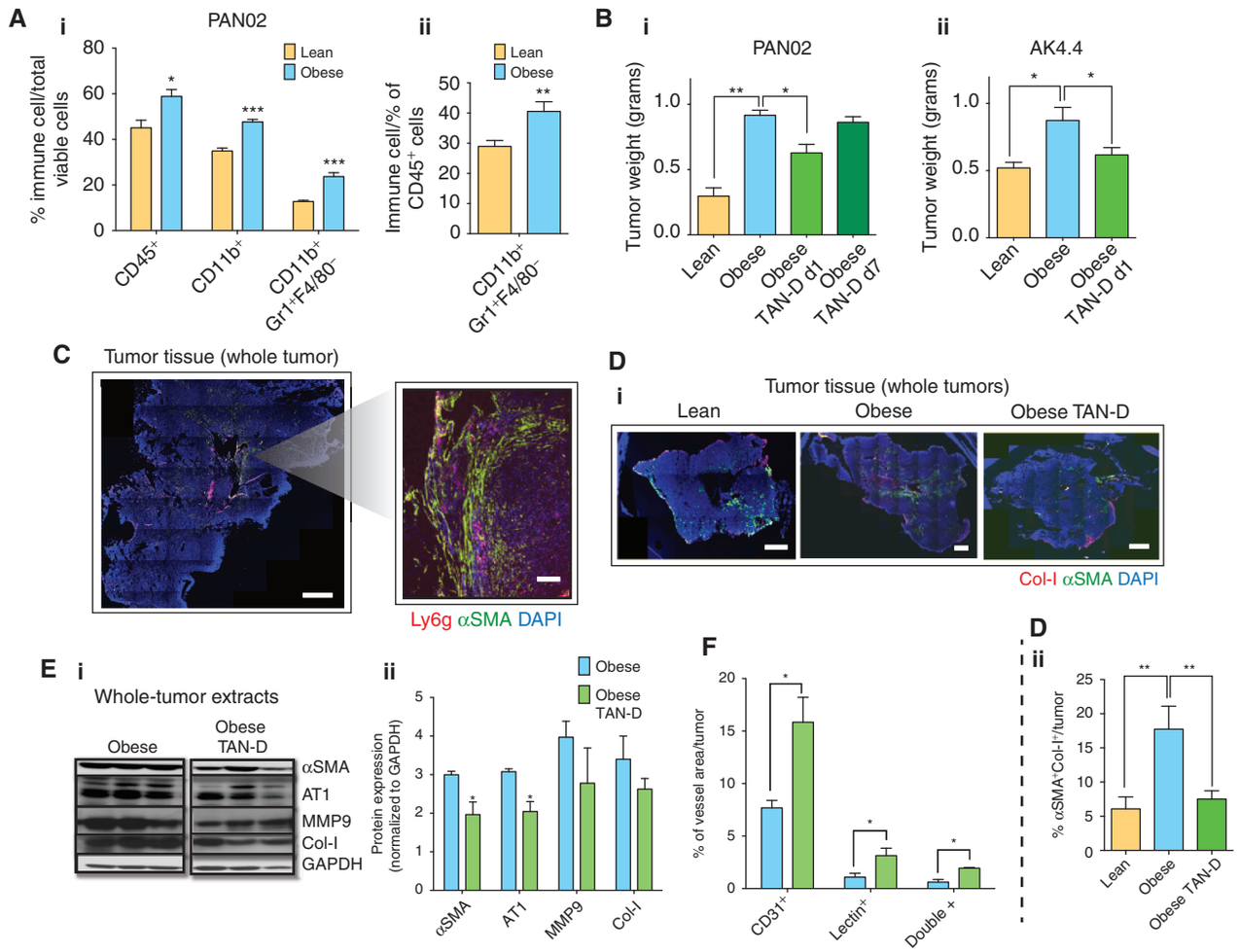

Figure 5. TANs mediate obesity-induced tumor progression and aggravated desmoplasia. **A,** effect of obesity on immune cell infiltration in PDACs. Obesity promoted infiltration of myeloid $CD11b^+Gr1^+F4/80^-$ cell population in PAN02 tumors in obese mice. Quantification normalized by total viable cells (**i**) or total CD45 leukocytes (**ii**; $n = 4$–6 tumors/group). **B,** effect of TAN-D on PDAC growth in obese mice. TAN-D from day 1 using anti-Ly6G-specific pharmacologic inhibitory antibody in obese mice significantly reverted the obesity-increased tumor weight in PAN02 and AK4.4 models ($n = 4$–6 tumors/group). **C,** preferential accumulation of TANs in areas with activated PSCs. Scale bars, 1 mm (whole tumors) and 100 μm (inset). **D,** TAN-D decreased activated PSCs in obese PDACs to the level of lean tumors. Representative pictures (**i**) and quantification of $\alpha SMA^+Col\text{-}I^+$ double-positive cells (**ii**; $n = 4$–6 tumors/group). **E,** TAN-D reduced AT1 expression, collagen production, and MMP9 expression in PAN02 tumors in obese animals. Representative Western blots (**i**) and quantification (**ii**) are shown. **F,** TAN-D led to increasing in perfusion in PAN02 tumors in obese animals. Percentage of $CD31^+$, $lectin^+$, or double-positive vessel density in the viable area of whole tumors ($n = 4$–6 tumors/group). Data are shown as mean ± SEM. *P* values were determined by the Student *t* test, or one-way ANOVA for **C** and **E**. *, $P < 0.05$; **, $P < 0.01$; *** $P < 0.001$.

for losartan in the AK4.4 tumor model (Supplementary Fig. S10Bi and S10Bii). The effects of AT1 blockade on the expression of IL1β and immune cell recruitment are consistent with the prevention of obesity-induced tumor growth (Fig. 4F) and indicate that AT1 signaling mediates obesity-augmented tumor progression via modulation of the immune microenvironment.

PDAC in Obese Patients Presents with Increased Adipocyte Area and Fibrosis

To validate the findings from mouse models of PDAC, we obtained samples of PDAC from treatment-naïve patients who presented with a body mass index (BMI) either below 25 (normal weight) or above 30 (obese). As in the mouse models, we found that tumors from obese patients presented with hypertrophic adipocytes (Fig. 7A) and more pronounced ECM deposition—as shown by increased collagen-I and HA expression (Fig. 7B).

Excess Weight in Patients with PDAC Is Associated with Worse Response to Chemotherapy

To validate our preclinical findings, we analyzed data collected from patients admitted to Massachusetts General Hospital (MGH) with a diagnosis of PDAC who underwent surgical resection. A total of 309 patients were included in this study. The average BMI of patients was 26.25 (BMI distribution in Supplementary Fig. S11). In normal-weight patients (BMI ≤ 25), adjuvant chemotherapy was a significant

Published OnlineFirst May 31, 2016; DOI: 10.1158/2159-8290.CD-15-1177

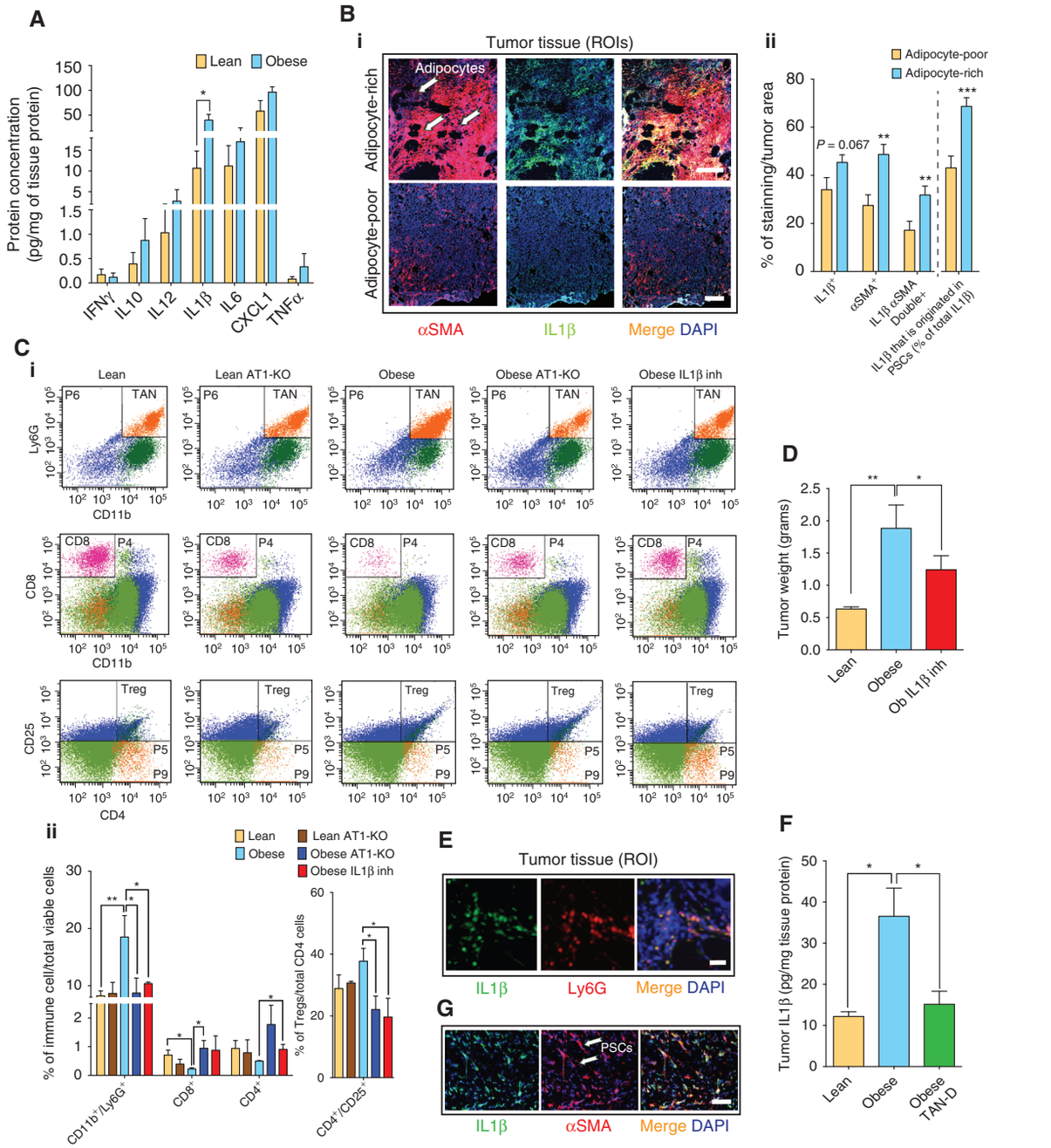

Figure 6. The adipose microenvironment promotes TAN infiltration and fibrosis via IL1β. **A,** effect of obesity on cytokine expression in PAN02 tumors. Multiplex protein revealed that PAN02 tumors from obese mice had increased expression of IL1β ($n = 4$–6 tumors/group). **B,** effect of adipocytes on IL1β and αSMA expression in PAN02 tumors. **Bi,** representative picture of αSMA and IL1β expression in adipocyte-rich and adipocyte-poor regions. Scale bars, 200 μm. **B-ii,** quantification of αSMA and IL1 β expression in adipocyte-rich and adipocyte-poor regions ($n = 20$ samples/region). IL1β was abundantly expressed in adipocytes and PSCs in the adipocyte-rich areas where PSCs predominate. **C,** effect of IL1β and AT1 blockade on immune cell profile. **Ci,** representative flow cytometry scatter plots of $CD45^+CD11b^+Ly6G^+$TANs, $CD8^+$ cytotoxic lymphocytes, and $CD4^+CD25^+$ Tregs in PAN02 tumors in lean and obese settings. Quantification normalized by total viable cells (**ii**) or total CD4 cells (**iii**; $n = 3$–6 tumors/group). Obesity promoted an increase in TANs, a decrease in $CD8^+$ lymphocytes, and a strong tendency for increased Tregs. An anti-IL1β neutralizing antibody (IL1β inh) or genetic AT1 blockade decreased $CD45^+CD11b^+Ly6G^+$ TAN infiltration while recovering $CD4^+$ and $CD8^+$ T cells (**i** and **ii**) and decreasing Tregs (**iii**) in obese mice (one-way ANOVA, $n = 3$–6 tumors/group). **D,** IL1β blockade normalized obesity-aggravated tumor growth (one-way ANOVA, $n = 3$–6 tumors/group). **E,** IL1β expression in TANs. Immunofluorescence for PAN02 tumor sections denoting colocalization. Scale bar, 30 μm. **F,** TAN-D using Ly6G-specific antibody abolished obesity-induced IL1β expression in PAN02 tumors (one-way ANOVA, $n = 4$–6 tumors/group). **G,** representative picture of αSMA and IL1β expression in PAN02 tumors. Scale bar, 30 μm. Data are shown as mean ± SEM. *P* values were determined by the Student *t* test unless otherwise stated. *, $P < 0.05$; **, $P < 0.01$; ***, $P < 0.001$.

Published OnlineFirst May 31, 2016; DOI: 10.1158/2159-8290.CD-15-1177

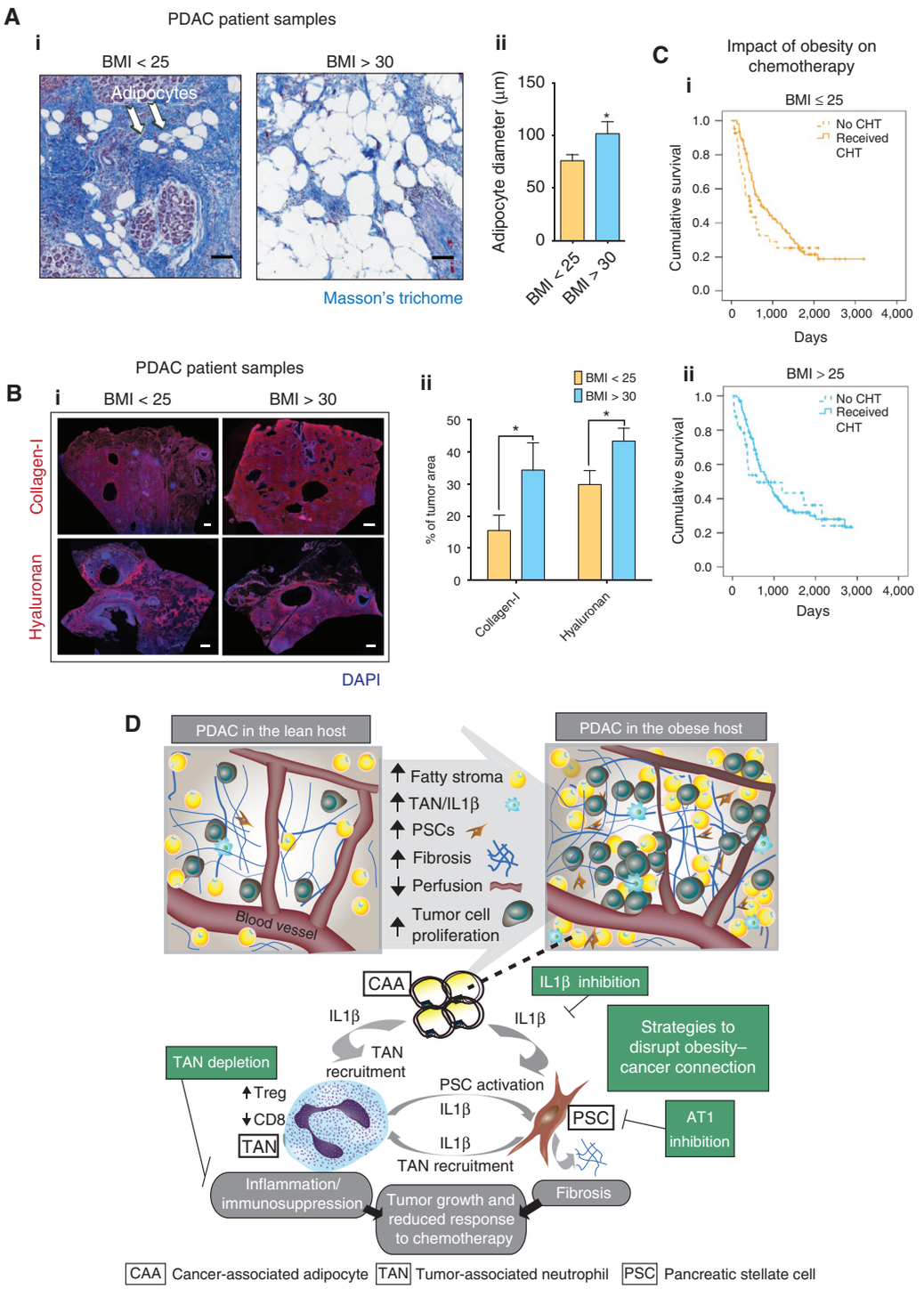

Figure 7. PDACs from obese patients recapitulate the findings in preclinical models. **A,** adipocytes in human PDACs in lean and obese patients. **Ai,** representative pictures of adipocytes in human PDAC from patients with normal weight (BMI < 25) and obesity (BMI > 30). Scale bars, 100 μm. **Aii,** quantification of adipocyte size in human PDACs. Tumors from obese patients presented with hypertrophied adipocytes ($n = 8$ tumors/group). **B,** collagen-I and HA expression in human PDACs in lean and obese patients. **Bi,** representative pictures of collagen-I and HA in human PDAC from patients with normal weight (BMI < 25) and obesity (BMI > 30). Scale bars, 1 mm. **Bii,** quantification of collagen-I and HA in human PDACs ($n = 8$ tumors/group). Obesity associated with increased levels of collagen-I and hyaluronan. **C,** cumulative survival curves in patients with PDAC stratified by chemotherapy (CHT) in patients with (**i**) BMI ≤ 25 or (**ii**) BMI >25. The survival advantage present in the BMI ≤ 25 subgroup is lost in the >25 BMI subgroup. **D,** graphical summary of the key findings of this study. PDACs in obese hosts present with increased fatty stroma, inflammation, and desmoplasia. The amplified cross-talk between CAAs, TANs, and PSCs that occurs in obesity leads to an aggravation of desmoplasia, increased tumor progression, and reduced response to chemotherapy.

Published OnlineFirst May 31, 2016; DOI: 10.1158/2159-8290.CD-15-1177

predictor of overall survival on multivariate analysis (HR, 0.5; 95% confidence interval, 0.3–0.8; $P < 0.005$), independent of other tumor characteristics including tumor size or lymph node positivity (Fig. 7Ci; Supplementary Tables S3 and S4). In overweight and obese patients (BMI > 25), we did not observe a significant survival advantage of adjuvant chemotherapy on either univariate or multivariate analysis (Fig. 7Cii; Supplementary Tables S5–S6). In conclusion, these results support our preclinical findings and suggest less efficacy of chemotherapy in overweight/obese patients. In conclusion, our preclinical and clinical studies indicate that excess weight alters the tumor microenvironment to augment the cross-talk between CAAs, TANs, and PSCs, which ultimately leads to increased tumor progression and reduced response to chemotherapy (Fig. 7D).

DISCUSSION

Obesity Promotes AT1-Dependent PSC Activation and PDAC Desmoplasia and Reduces the Efficacy of 5-FU Chemotherapy

We and others have shown that obesity promotes pancreatic tumor initiation, growth, and metastasis in preclinical models (27, 30, 41–44). Here, we show in established PDAC models that obesity stimulates the activity of IL1β and the cross-talk between adipocytes, TANs, and PSCs to worsen the fibroinflammatory microenvironment. The increased fibroinflammatory activity then promotes tumor progression and reduces vascular perfusion, drug delivery, and the efficacy of chemotherapy. We also uncovered that AT1 signaling can mediate obesity-induced PSC activation and increase collagen-I accumulation. The inhibition of AT1 signaling is particularly effective in preventing these effects in obese animals, reverting the obesity-accelerated tumor progression and resensitizing tumors to the chemotherapeutic agent 5-FU in obese mice.

In Obese Mice, the Abundance of Adipocytes and TANs Increases PSC Activation via IL1β Particularly in Adipocyte-Rich Regions

In more than half of patients with PDAC, adipocytes infiltrate >20% of pancreatic tissue (28). Similar to previous reports (27, 28, 45), we demonstrated that hypertrophic tumor adipocytes—referred to as cancer-associated adipocytes (CAA; refs. 45, 46)—accumulate in murine and human PDAC in the obese setting. It is well known that obesity promotes the secretion of inflammatory cytokines from hypertrophic adipocytes in adipose tissues and the pancreas, which ultimately leads to local tissue fibrosis (21, 22, 25, 47, 48). However, how hypertrophic CAAs facilitate the interaction between inflammation and desmoplasia to ultimately promote PDAC progression in the obese setting was unknown. We observed here an accumulation of activated PSCs and fibrosis surrounding CAA-rich areas. Given the increased adipocyte burden, the overall PSC activation and fibrotic content in tumors were consequently increased. We also found in obese mice that CAAs express IL1β, which increases the production of IL1β in PDAC, especially in CAA-rich areas. In line with IL1β being an activator of PSCs (49), we found that IL1β inhibition reduces PSC activation in PDACs in obese animals, indicating that the elevated production of IL1β in CAA-rich regions leads to activation of PSCs. This is in agreement with previous reports showing that in the pancreas of mice fed a high-fat diet, fibrosis is also accompanied by inflammation in early-stage neoplastic lesions (43, 44), and with our previous observation that metformin reduces IL1β and desmoplasia in tumors implanted in obese mice (50). It was shown before that neutrophil infiltrates can be observed in the vicinity of tumor cells and in the desmoplastic tumor stroma, which correlates with undifferentiated tumor growth and poor prognosis (51). We found that TAN-specific depletion reduces PSC activation and the number of αSMA-positive cells associated with collagen-I. In addition, we discovered that IL1β could recruit/activate TANs. This is consistent with previous reports of increased levels of myeloperoxidase—a marker of intrapancreatic neutrophil sequestration/activation—associating with IL1β in the steatotic pancreas of obese mice (25, 52). Furthermore, our results show that TANs also secrete IL1β, which may then activate PSCs and further increase TAN recruitment. Our results explain the findings that, in patients with pancreatic cancer, the intrapancreatic fat correlates with the increased incidence of PDAC and lymphatic metastasis, and decreased survival (28, 53). In conclusion, in obese mice, the cross-talk between adipocytes, TANs, and PSCs—mediated in part by IL1β—stimulates the activation of PSCs.

Obesity-Induced TAN Recruitment and IL1β Promote Immunosuppression and the Growth of PDAC

We also found here that TAN-D in obese mice reduced tumor growth, which is consistent with the correlation between TAN infiltration and more aggressive types of pancreatic tumors (54). Importantly, the obesity-induced increase in TANs occurred concomitantly with decreased $CD8^+$ T cells and increased Tregs, which is typical of an immunosuppressive microenvironment that promotes tumor progression (55, 56). In fact, we previously found that obesity is associated with an increased expression of the immunosuppressive molecules IL4 and IL5 in PAN02 tumors (30), which was confirmed here in the AK4.4 model (Supplementary Fig. S8B). Furthermore, we found here that IL1β inhibition recapitulates the effect of TAN-D on the immune phenotype and tumor growth, consistent with the TAN-recruiting effect of IL1β. These findings extend our previous observations that obesity is associated with inflammation, immunosuppression, and macrophage recruitment in PAN02 tumors, and that reducing IL1β production via VEGFR1 inhibition leads to a reduction in tumor progression in obese mice (30). Considering that the immune environment in obesity appears to be suppressed, and the unprecedented success of therapies that block immune checkpoint pathways (55), it would be interesting to evaluate whether these therapies will be particularly effective in obese hosts.

Obesity Promotes the Cross-talk between CAAs, TANs, and PSCs That Leads to PDAC Growth

We found that the reduction in PSC activation after AT1 blockade, in addition to decreasing obesity-associated desmoplasia, also reduces the levels of IL1β, decreases the

Published OnlineFirst May 31, 2016; DOI: 10.1158/2159-8290.CD-15-1177

infiltration of TANs and Tregs, increases the number of $CD8^+$ T cells, and reduces obesity-associated tumor growth. These findings suggest that the interaction of inflammatory cells and PSCs is bidirectional—targeting TANs reduces PSC activation, and, in turn, targeting PSCs reduces the recruitment of TANs, with both approaches reducing tumor growth. This is consistent with previous *in vitro* work demonstrating that neutrophils interact reciprocally with myofibroblasts and PSCs (57, 58). In conclusion, our work reveals a cross-talk between CAAs, TANs, and PSCs that promotes tumor progression in obese hosts, with IL1β (secreted by all these cells) playing a major role in this cooperation (Fig. 7D).

AT1 Inhibition Reverses Obesity-Induced PDAC Growth

Similar to our previous results in mice fed a regular diet (18), losartan or AT1 deletion did not affect the growth of PDAC in lean mice. In contrast, in obese animals AT1 inhibition reduced PDAC growth, which was likely due to the inhibition of the protumorigenic activity of TANs and IL1β, which modulate the recruitment/activity of CD8-positive T cells and Tregs, as discussed above. The reduction of TAN recruitment after AT1 inhibition may result from a direct effect, because neutrophils have been shown to express AT1 (59, 60). Indeed, we found that approximately 40% of TANs expressed AT1 in the PAN02 model (Supplementary Fig. S12) and similarly in AK4.4 and KPC models (data not shown). Alternatively, the effects of AT1 blockade on immune cell recruitment could also be indirect. We showed that IL1β recruits TANs, and AT1 inhibition reduced the production of IL1β. This could be due to AT1 inhibition of PSCs or tumor adipocytes, as both cells express AT1 and produce IL1β. In fact, AT1 is highly expressed in normal adipocytes (23), its activity is increased in adipose tissues in obesity (23, 24), and we show here that it is expressed in CAA as well (Supplementary Fig. S13). Moreover, AT1 deletion reduced the levels of the TAN chemoattractant CXCL1 and the TAN activation molecule INFγ in tumors (Supplementary Fig. S14A), which can also explain the reduced TAN infiltration.

On the other hand, AT1 inhibition in obese mice reduced the expression of hypoxia and EMT markers in tumors (Supplementary Figs. S3E and S14B), likely due to its effects on the desmoplastic microenvironment (Supplementary Fig. S3E). These effects of AT inhibition may have also contributed to the reduction of tumor progression in obesity. In addition, obesity also increased AKT/ERK, p38, JNK, and pS6/4EBP1 signaling, which is involved not only in AT1 signaling/desmoplasia in PSCs, but also in proliferation and survival of PDAC cells (61–63). Because losartan reduced the activation of some of these signaling pathways (p38/JNK/4EBP1), its effects on tumor growth may also be explained by a direct effect on cell proliferation/survival.

AT1 Ablation Reverses Obesity-Induced Chemoresistance

In contrast to the antitumor effects of losartan, 5-FU reduced PDAC growth in lean but not obese mice, which could be due to the significantly lower intratumoral vascular perfusion and 5-FU uptake in obese than lean mice. In obese mice, AT1 deletion significantly increased the antitumor activity of 5-FU, whereas the effect of the combination of losartan and 5-FU was not superior to 5-FU alone. In fact, and in contrast to our previous study (18), the increased 5-FU activity induced by losartan was not related to a significant increase in vascular perfusion or drug uptake. Blood flow in tumors is known to be highly dependent on the MABP (64); thus, it is possible that the significant decrease in MABP induced by the relatively high dose of losartan (90 mg/kg) may have affected the tumor blood flow, thus minimizing the positive effects of losartan on vascular perfusion. Apart from the effects of losartan on TANs or the adaptive immune response, the losartan-induced decrease in SNAIL expression and phospho-p38 may also increase the cytotoxic activity of 5-FU. p38 is known to be involved in chemoresistance (65), and in mouse models of pancreatic cancer, SNAIL deletion increased the antitumor activity of gemcitabine (66).

Of note, consistent with previous work in PAN02 tumors (67), by using both genetic and diet-induced obese mouse models we determined that obesity promotes tumor growth independent of diet. This was also confirmed by the finding that FVB mice that did not gain weight despite an HFD (~25% of all mice on an HFD) were observed to have tumor growth similar to that in lean animals (not shown).

Validation of Preclinical Findings in Patients with PDAC

We found that our key observations in mice were also present in patients. In particular, excess weight was associated with increased number and size of adipocytes and desmoplasia in tumors and reduced response to chemotherapy. Although the specific effect of obesity on patients with PDAC in a neoadjuvant setting is not known, we found that obesity adversely affected patients with PDAC who received adjuvant chemotherapy. Moreover, the high incidence (~85% in our cohort; Supplementary Fig. S15) of hypertension in obese patients makes it an ideal target population for AT1 inhibitors (ACERi/ARBs), considering the blood pressure–lowering effect of these drugs.

CONCLUSIONS

Obesity is considered to be responsible for 14% to 20% of all cancer-related deaths in the United States (4). As a result, the obesity epidemic—which also affects the majority of patients with PDAC—highlights the importance of understanding the pathophysiology underlying the obesity–cancer connection. We had previously found that obesity associates with increased tumor inflammation, immune cell recruitment, and tumor growth. We discovered here that obesity-induced inflammation and TAN infiltration lead to a desmoplastic tumor microenvironment, which directly promotes tumor growth and impairs the response to chemotherapy. Both of these factors may explain the poor outcomes in obese patients. The finding that obesity-induced desmoplasia responds to clinically available antifibrotic therapies (e.g., ARBs) is extremely encouraging and strongly supports the implementation of clinical trials to determine the efficacy of these therapies in obese patients with PDAC in combination with the current standard of care. Because epidemiologic and molecular evidence suggests a link between obesity and other desmoplastic cancer types, the strategies established in this study may also apply to

Published OnlineFirst May 31, 2016; DOI: 10.1158/2159-8290.CD-15-1177

a broader patient population. In conclusion, obesity and the obesity-related markers described here (increased desmoplasia, TAN infiltration, and IL1β expression) may help explain the poorer prognosis in patients with PDAC.

METHODS

Obese Mouse Models

C57BL/6 WT, leptin-deficient (*ob/ob*), AT1-knockout (KO; *agtr1a*$^{-/-}$) or AT2-KO (*agtr2*$^{-/-}$; all C57BL/6 background), and FVB mice were originally obtained from The Jackson Laboratory and bred and maintained in our defined flora animal colony. KPC (PTF1-Cre/LSL-KRAS^{G12D}/p53-R172H, mixed C57BL/6 and FVB background) and iKRAS (p48-Cre;R26-rtTa-IRES-EGFP;TetO-Kras^{G12D} mice, FVB background; refs. 32–35, 68) mice were obtained from our collaborators. To generate an obese model, mice (6 weeks old) were given either a 10% or a 60% fat diet (D12450J and D12492; Research Diets) for 10 weeks (or until tumor collection in KPC spontaneous models), as previously described (68–70). iKRAS mice were given 10% and 60% doxycycline (650 mg/kg)–containing diet for induction of PDAC development (D14071902 and D14071903; Research Diets). *ob/ob* mice remained on standard chow. For implanted tumor experiments, AK4.4 cells (KRAS^{G12D} and p53$^{+/-}$) were kindly provided by Dr. Nabeel Bardeesy and were isolated from mice generating spontaneous pancreatic tumors (PTF1-Cre/LSL-KRAS^{G12D}/p53$^{lox/+}$; ref. 71). PAN02 cells (*SMAD4-m174*; ref. 72) were obtained from the ATCC. Orthotopic pancreatic tumors were generated by implanting a small piece (1 mm^3) of viable tumor tissue (from a source tumor in a separate donor animal) into the pancreas of 6-to-8-week-old male lean or obese FVB (AK4.4 model) or C57BL/6 background (PAN02 model) mice. PAN02 tumor chunks and AK4.4 cells were authenticated by IDEXX laboratories (PAN02: IDEXX RADIL Case # 22366, 2013; AK4.4: IDEXX RADIL Case # 27818, 2014; please see more details in Supplementary Methods). With exception of PAN02, these orthotopically grown pancreatic cancers are characterized by a dense collagenous stroma, a hallmark of pancreatic cancer desmoplasia (73). All experimental uses of animals abide by the Public Health Service Policy on Humane Care of Laboratory Animals and were approved by the Institutional Animal Care and Use Committee at Massachusetts General Hospital.

Pancreatic Tumor Growth Studies

For all experiments unless specified below, mice bearing orthotropic PAN02 or AK4.4 pancreatic tumors were randomized into treatment groups (or controls), and tumors were collected at day 21 after implantation. For the tumor growth study with chemotherapy, mice were divided into treatment groups 7 days after implantation when tumors in lean and obese mice had similar sizes, as determined by ultrasound (Supplementary Fig. S5J), and treated with either 5-FU (30 mg/kg i.v. every 4 days) or an equal volume of saline by intravenous injection on days 7, 11, and 15 after implantation, with tumors collected at day 19. For the tumor growth study with losartan, mice were treated with losartan (90 mg/kg i.p. every day) or an equal volume of PBS intraperitoneally starting on day 5 after implantation for the duration of the study. In the combined experiment of losartan and 5-FU, the same protocol was used for each drug as described above. TAN-D by a Ly6G-specific inhibitor (BioExcell; 4 mg/Kg i.p. every 2 days) was administered starting at day 1 or day 7. IL1β inhibition (MM425B; Endogen/Pierce Biotechnology; 2 mg/kg i.p. every 2 days) was administered to PAN02-bearing animals starting at day 7. At the completion of the study, adipose tissue and tumor samples were collected, weighed, and processed for further analysis (for information on rtPCRarray, immunohistochemistry/immunofluorescence, Western blotting, ELISA, and flow cytometry, please see Supplementary Methods). When spontaneous models were used, tumors were collected when palpable. For drug delivery in tumors, drug preparation, and ultrasound and blood pressure measurements, please refer to Supplementary Methods.

Human Samples/Clinical Studies

Human samples of pancreatic cancer were obtained from the MGH tissue repository. Tumors selected received no prior chemotherapy or radiotherapy before the surgical specimen was collected at the time of tumor resection. BMI was obtained for the respective sample. A total of 16 samples were randomly selected from this subset of samples (8 with BMI < 25 and 8 with BMI > 30). Paraffin sections were stained for collagen-I and HA as described below. Images were acquired using confocal microscopy and quantified using Matlab. Data were analyzed anonymously. For survival studies, 309 consecutive patients with pancreatic cancer who received surgical resection who were followed up in MGH between 2006 and 2010 with information including clinicopathologic details, treatment received, and BMI at the time of diagnosis were included. Written informed consent from the patient or the next of kin was obtained for the use of pancreatic cancer samples or clinical data. All studies were conducted in accordance with the Declaration of Helsinki and were approved by an Institutional Review Board. All patients have a pathology-confirmed diagnosis of PDAC.

Statistical Analysis

Statistical analyses were performed using GraphPad Prism Version 6.0f (GraphPad Software) and SPSS software (for clinical studies), version 22 (SPSS). Error bars indicate the SEM of data from replicate experiments. The significance of difference between samples within figures was confirmed using unpaired *t* tests, one-way ANOVA, χ^2 test, or two-way ANOVA, depending on the experimental setting. In clinical studies, patients were divided into BMI ≤ 25 (n = 145), or BMI > 25 (n = 164), with mean BMI being 26.25. The values of BMI represent the BMI at the time of diagnosis. Overall survival was defined as the time from date of diagnosis until date of death or last contact. Survival curves were calculated using Kaplan–Meier methods and were compared using the log-rank test. Covariates with a P value < 0.150 in univariate analysis were included into multivariate analyses. Cox proportional hazards regression analyses were used to conduct comparisons for chemotherapy efficacy. The association of adjuvant chemotherapy and overall survival was adjusted for tumor size (continuous variable), lymph vessel and perineural invasion (absent vs. present), lymph nodes (negative vs. positive), surgical margin (negative vs. positive), pathologic grading (1–2 vs. 3–4), adjuvant radiation (yes vs. no), and adjuvant chemotherapy (yes vs. no). Time to event was diagnosis of pancreatic cancer until death or last follow-up with individuals still alive at last follow-up being coded as censored for the event (death) as of that date. For comparison between prevalence of hypertension, a χ^2 test was performed. In all analyses, a P value of less than 0.05 was considered significant.

Disclosure of Potential Conflicts of Interest

V.P. Chauhan has ownership interest (including patents) in XTuit Pharmaceuticals. Y. Boucher is a consultant for Xtuit Inc. R.K. Jain received consultant fees from Ophthotech, SPARC, SynDevRx, and XTuit. R.K. Jain owns equity in Enlight, Ophthotech, SynDevRx, and XTuit and serves on the Board of Directors of XTuit and the Boards of Trustees of Tekla Healthcare Investors, Tekla Life Sciences Investors, Tekla Healthcare Opportunities Fund, and Tekla World Healthcare Fund. No reagents or funding from these companies was used in these studies. R.K. Jain, J. Incio, and D. Fukumura have ownership interest in a provisional patent application filed December 18, 2015, titled "Polyacetal Polymers, Conjugates, Particles and Uses Thereof." No potential conflicts of interest were disclosed by the other authors.

Published OnlineFirst May 31, 2016; DOI: 10.1158/2159-8290.CD-15-1177

Authors' Contributions

Conception and design: J. Incio, I.X. Chen, V. Desphande, Y. Boucher, D. Fukumura, R.K. Jain
Development of methodology: J. Incio, I.X. Chen, Y. Huang, P. Huang, V. Desphande, D. Fukumura
Acquisition of data (provided animals, acquired and managed patients, provided facilities, etc.): J. Incio, H. Liu, P. Suboj, I.X. Chen, M.R. Ng, H.T. Nia, S. Kao, S. Babykutty, Y. Huang, K. Jung, N.N. Rahbari, J. Kahn, V. Desphande, J. Michaelson, T.P. Michelakos, D. Fukumura, R.K. Jain
Analysis and interpretation of data (e.g., statistical analysis, biostatistics, computational analysis): J. Incio, H. Liu, P. Suboj, S.M. Chin, I.X. Chen, M. Pinter, H.T. Nia, S. Kao, S. Babykutty, Y. Huang, N.N. Rahbari, X. Han, V.P. Chauhan, J.D. Martin, V. Desphande, T.P. Michelakos, Y. Boucher, D. Fukumura, R.K. Jain
Writing, review, and/or revision of the manuscript: J. Incio, H. Liu, P. Suboj, I.X. Chen, M. Pinter, M.R. Ng, J. Grahovac, S. Kao, S. Babykutty, N.N. Rahbari, V.P. Chauhan, J.D. Martin, J. Kahn, V. Desphande, T.P. Michelakos, C.R. Ferrone, R. Soares, Y. Boucher, D. Fukumura, R.K. Jain
Administrative, technical, or material support (i.e., reporting or organizing data, constructing databases): J. Incio, S.M. Chin, M. Pinter, J. Grahovac, J. Kahn, P. Huang, D. Fukumura, R.K. Jain
Study supervision: J. Incio, D. Fukumura, R.K. Jain
Other (performed the animal surgery): J. Kahn

Acknowledgments

The authors thank Sylvie Roberge for assistance with tumor implantation and blood pressure measurements, Sergey Kozin for assistance with blood pressure measurements, Penny Woo for assistance with animal husbandry, Carolyn Smith for assistance with immunohistochemical studies, Lance Munn for his contribution to illustrations, and Ana Batista and Peter Blume-Jensen for suggestions and critiques to the manuscript.

Grant Support

This study was supported in part by the NIH (CA80124, CA85140, CA96915, CA115767, and CA126642 to R.K. Jain and D. Fukumura), the Lustgarten Foundation (research grant to R.K. Jain), the Foundation for Science and Technology (Portugal, POPH/FSE funding program, fellowship and research grant to J. Incio), and the Austrian Science Fund (FWF), project number J3747-B28 (to M. Pinter).

Received September 28, 2015; revised May 16, 2016; accepted May 23, 2016; published OnlineFirst May 31, 2016.

REFERENCES

1. American Cancer Society. Cancer Facts & Figures 2015. Atlanta: American Cancer Society; 2015.
2. Genkinger JM, Spiegelman D, Anderson KE, Bernstein L, van den Brandt PA, Calle EE, et al. A pooled analysis of 14 cohort studies of anthropometric factors and pancreatic cancer risk. Int J Cancer 2011;129:1708–17.
3. Yuan C, Bao Y, Wu C, Kraft P, Ogino S, Ng K, et al. Prediagnostic body mass index and pancreatic cancer survival. J Clin Oncol 2013;31:4229–34.
4. Calle EE, Rodriguez C, Walker-Thurmond K, Thun MJ. Overweight, obesity, and mortality from cancer in a prospectively studied cohort of U.S. adults. N Engl J Med 2003;348:1625–38.
5. McWilliams RR, Matsumoto ME, Burch PA, Kim GP, Halfdanarson TR, de Andrade M, et al. Obesity adversely affects survival in pancreatic cancer patients. Cancer 2010;116:5054–62.
6. Li D, Morris JS, Liu J, Hassan MM, Day RS, Bondy ML, et al. Body mass index and risk, age of onset, and survival in patients with pancreatic cancer. JAMA 2009;301:2553–62.
7. Smits MM, van Geenen EJ. The clinical significance of pancreatic steatosis. Nat Rev Gastroenterol Hepatol 2011;8:169–77.
8. Ogden CL, Carroll MD, Kit BK, Flegal KM. Prevalence of childhood and adult obesity in the United States, 2011–2012. JAMA 2014;311:806–14.
9. Dvorak HF. Tumors: Wounds that do not heal. Similarities between tumor stroma generation and wound healing. N Engl J Med 1986;315:1650–9.
10. Whatcott CJ, Diep CH, Jiang P, Watanabe A, LoBello J, Sima C, et al. Desmoplasia in primary tumors and metastatic lesions of pancreatic cancer. Clin Cancer Res 2015;21:3561–8.
11. Olive KP, Jacobetz MA, Davidson CJ, Gopinathan A, McIntyre D, Honess D, et al. Inhibition of Hedgehog signaling enhances delivery of chemotherapy in a mouse model of pancreatic cancer. Science 2009;324:1457–61.
12. Hwang RF, Moore T, Arumugam T, Ramachandran V, Amos KD, Rivera A, et al. Cancer-associated stromal fibroblasts promote pancreatic tumor progression. Cancer Res 2008;68:918–26.
13. Neesse A, Frese KK, Bapiro TE, Nakagawa T, Sternlicht MD, Seeley TW, et al. CTGF antagonism with mAb FG-3019 enhances chemotherapy response without increasing drug delivery in murine ductal pancreas cancer. Proc Natl Acad Sci U S A 2013;110:12325–30.
14. Stylianopoulos T, Martin JD, Chauhan VP, Jain SR, Diop-Frimpong B, Bardeesy N, et al. Causes, consequences, and remedies for growth-induced solid stress in murine and human tumors. Proc Natl Acad Sci U S A 2012;109:15101–8.
15. Chauhan VP, Boucher Y, Ferrone CR, Roberge S, Martin JD, Stylianopoulos T, et al. Compression of pancreatic tumor blood vessels by hyaluronan is caused by solid stress and not interstitial fluid pressure. Cancer Cell 2014;26:14–5.
16. Alvarez R, Musteanu M, Garcia-Garcia E, Lopez-Casas PP, Megias D, Guerra C, et al. Stromal disrupting effects of nab-paclitaxel in pancreatic cancer. Br J Cancer 2013;109:926–33.
17. Hidalgo M, Von Hoff DD. Translational therapeutic opportunities in ductal adenocarcinoma of the pancreas. Clin Cancer Res 2012;18:4249–56.
18. Chauhan VP, Martin JD, Liu H, Lacorre DA, Jain SR, Kozin SV, et al. Angiotensin inhibition enhances drug delivery and potentiates chemotherapy by decompressing tumor blood vessels. Nat Commun 2013;4:2516.
19. Endrich B, Reinhold HS, Gross JF, Intaglietta M. Tissue perfusion inhomogeneity during early tumor growth in rats. J Natl Cancer Inst 1979;62:387–95.
20. Costa C, Incio J, Soares R. Angiogenesis and chronic inflammation: cause or consequence? Angiogenesis 2007;10:149–66.
21. Hosogai N, Fukuhara A, Oshima K, Miyata Y, Tanaka S, Segawa K, et al. Adipose tissue hypoxia in obesity and its impact on adipocytokine dysregulation. Diabetes 2007;56:901–11.
22. Gonzalez-Perez RR, Rueda BR. Tumor angiogenesis regulators. Boca Raton: Taylor & Francis; 2013.
23. AGTR1 (angiotensin II receptor, type 1) gene expression. Biogps.org (http://biogps.org/#goto=genereport&id=185). In Wu C, Orozco C, Boyer J, Leglise M, Goodale J, Batalov S, et al. BioGPS: an extensible and customizable portal for querying and organizing gene annotation resources. Genome Biol 2009;10:R130.
24. Sun K, Tordjman J, Clement K, Scherer PE. Fibrosis and adipose tissue dysfunction. Cell Metab 2013;18:470–7.
25. Mathur A, Marine M, Lu D, Swartz-Basile DA, Saxena R, Zyromski NJ, et al. Nonalcoholic fatty pancreas disease. HPB (Oxford) 2007;9:312–8.
26. Matsuda A, Makino N, Tozawa T, Shirahata N, Honda T, Ikeda Y, et al. Pancreatic fat accumulation, fibrosis, and acinar cell injury in the Zucker diabetic fatty rat fed a chronic high-fat diet. Pancreas 2014;43:735–43.
27. Zyromski NJ, Mathur A, Pitt HA, Wade TE, Wang S, Nakshatri P, et al. Obesity potentiates the growth and dissemination of pancreatic cancer. Surgery 2009;146:258–63.

28. Hori M, Takahashi M, Hiraoka N, Yamaji T, Mutoh M, Ishigamori R, et al. Association of pancreatic Fatty infiltration with pancreatic ductal adenocarcinoma. Clin Translat Gastroenterol 2014;5:e53.
29. Hefetz-Sela S, Scherer PE. Adipocytes: Impact on tumor growth and potential sites for therapeutic intervention. Pharmacol Therapeut 2013;138:197–210.
30. Incio J, Tam J, Rahbari NN, Suboj P, McManus DT, Chin SM, et al. PlGF/VEGFR-1 signaling promotes macrophage polarization and accelerated tumor progression in obesity. Clin Cancer Res 2016;22:2993–3004.
31. Bracci PM. Obesity and pancreatic cancer: Overview of epidemiologic evidence and biologic mechanisms. Mol Carcinog 2012;51:53–63.
32. Hingorani SR, Wang L, Multani AS, Combs C, Deramaudt TB, Hruban RH, et al. Trp53R172H and KrasG12D cooperate to promote chromosomal instability and widely metastatic pancreatic ductal adenocarcinoma in mice. Cancer cell 2005;7:469–83.
33. Kawaguchi Y, Cooper B, Gannon M, Ray M, MacDonald RJ, Wright CV. The role of the transcriptional regulator Ptf1a in converting intestinal to pancreatic progenitors. Nature genetics 2002;32:128–34.
34. Kanasaki K, Koya D. Biology of obesity: Lessons from animal models of obesity. J Biomed Biotechnol 2011;2011:197636.
35. Collins MA, Bednar F, Zhang Y, Brisset JC, Galban S, Galban CJ, et al. Oncogenic Kras is required for both the initiation and maintenance of pancreatic cancer in mice. J Clin Invest 2012;122:639–53.
36. Neoptolemos JP, Moore MJ, Cox TF, Valle JW, Palmer DH, McDonald AC, et al. Effect of adjuvant chemotherapy with fluorouracil plus folinic acid or gemcitabine vs observation on survival in patients with resected periampullary adenocarcinoma: the ESPAC-3 periampullary cancer randomized trial. JAMA 2012;308:147–56.
37. Yang F, Chung AC, Huang XR, Lan HY. Angiotensin II induces connective tissue growth factor and collagen I expression via transforming growth factor-beta-dependent and -independent Smad pathways: The role of Smad3. Hypertension 2009;54:877–84.
38. Hama K, Ohnishi H, Yasuda H, Ueda N, Mashima H, Satoh Y, et al. Angiotensin II stimulates DNA synthesis of rat pancreatic stellate cells by activating ERK through EGF receptor transactivation. Biochem Biophys Res Commun 2004;315:905–11.
39. Hama K, Ohnishi H, Aoki H, Kita H, Yamamoto H, Osawa H, et al. Angiotensin II promotes the proliferation of activated pancreatic stellate cells by Smad7 induction through a protein kinase C pathway. Biochem Biophys Res Commun 2006;340:742–50.
40. Weisberg SP, McCann D, Desai M, Rosenbaum M, Leibel RL, Ferrante AW Jr. Obesity is associated with macrophage accumulation in adipose tissue. J Clin Invest 2003;112:1796–808.
41. Fukumura D, Incio J, Shankaraiah RC, Jain RK. Obesity and cancer: An angiogenic and inflammatory link. Microcirculation 2016;23:191–206.
42. White PB, True EM, Ziegler KM, Wang SS, Swartz-Basile DA, Pitt HA, et al. Insulin, leptin, and tumoral adipocytes promote murine pancreatic cancer growth. J Gastroint Surg 2010;14:1888–93; discussion 93–4.
43. Philip B, Roland CL, Daniluk J, Liu Y, Chatterjee D, Gomez SB, et al. A high-fat diet activates oncogenic Kras and COX2 to induce development of pancreatic ductal adenocarcinoma in mice. Gastroenterology 2013;145:1449–58.
44. Khasawneh J, Schulz MD, Walch A, Rozman J, Hrabe de Angelis M, Klingenspor M, et al. Inflammation and mitochondrial fatty acid beta-oxidation link obesity to early tumor promotion. Proc Natl Acad Sci U S A 2009;106:3354–9.
45. Dirat B, Bochet L, Dabek M, Daviaud D, Dauvillier S, Majed B, et al. Cancer-associated adipocytes exhibit an activated phenotype and contribute to breast cancer invasion. Cancer Res 2011;71:2455–65.
46. Wang YY, Lehuede C, Laurent V, Dirat B, Dauvillier S, Bochet L, et al. Adipose tissue and breast epithelial cells: A dangerous dynamic duo in breast cancer. Cancer Lett 2012;324:142–51.
47. Hursting SD. Minireview: The year in obesity and cancer. Mol Endocrinol 2012;26:1961–6.
48. Hursting SD, Dunlap SM. Obesity, metabolic dysregulation, and cancer: A growing concern and an inflammatory (and microenvironmental) issue. Ann N Y Acad Sci 2012;1271:82–7.
49. Masamune A, Satoh M, Kikuta K, Sakai Y, Satoh A, Shimosegawa T. Inhibition of p38 mitogen-activated protein kinase blocks activation of rat pancreatic stellate cells. J Pharmacol Exp Ther 2003;304:8–14.
50. Incio J, Suboj P, Chin SM, Vardam-Kaur T, Liu H, Hato T, et al. Metformin reduces desmoplasia in pancreatic cancer by reprogramming stellate cells and tumor-associated macrophages. PloS One 2015;10:e0141392.
51. Felix K, Gaida MM. Neutrophil-derived proteases in the microenvironment of pancreatic cancer -active players in tumor progression. Int J Biol Sci 2016;12:302–13.
52. Zyromski NJ, Mathur A, Pitt HA, Lu D, Gripe JT, Walker JJ, et al. A murine model of obesity implicates the adipokine milieu in the pathogenesis of severe acute pancreatitis. Am J Physiol Gastrointest Liver Physiol 2008;295:G552–8.
53. Mathur A, Zyromski NJ, Pitt HA, Al-Azzawi H, Walker JJ, Saxena R, et al. Pancreatic steatosis promotes dissemination and lethality of pancreatic cancer. J Am Coll Surg 2009;208:989–94; discussion 94–6.
54. Reid MD, Basturk O, Thirabanjasak D, Hruban RH, Klimstra DS, Bagci P, et al. Tumor-infiltrating neutrophils in pancreatic neoplasia. Mod Pathol 2011;24:1612–9.
55. Coussens LM, Zitvogel L, Palucka AK. Neutralizing tumor-promoting chronic inflammation: A magic bullet? Science 2013;339:286–91.
56. Fridlender ZG, Sun J, Kim S, Kapoor V, Cheng G, Ling L, et al. Polarization of tumor-associated neutrophil phenotype by TGF-beta: "N1" versus "N2" TAN. Cancer Cell 2009;16:183–94.
57. Chrysanthopoulou A, Mitroulis I, Apostolidou E, Arelaki S, Mikroulis D, Konstantinidis T, et al. Neutrophil extracellular traps promote differentiation and function of fibroblasts. J Pathol 2014;233:294–307.
58. Zhu Q, Zhang X, Zhang L, Li W, Wu H, Yuan X, et al. The IL-6-STAT3 axis mediates a reciprocal crosstalk between cancer-derived mesenchymal stem cells and neutrophils to synergistically prompt gastric cancer progression. Cell Death Dis 2014;5:e1295.
59. Raiden S, Pereyra Y, Nahmod V, Alvarez C, Castello L, Giordano M, et al. Losartan, a selective inhibitor of subtype AT1 receptors for angiotensin II, inhibits neutrophil recruitment in the lung triggered by fMLP. J Leukoc Biol 2000;68:700–6.
60. Raiden S, Giordano M, Andonegui G, Trevani AS, Lopez DH, Nahmod V, et al. Losartan, a selective inhibitor of subtype AT1 receptors for angiotensin II, inhibits the binding of N-formylmethionyl-leucyl-phenylalanine to neutrophil receptors. J Pharmacol Exp Ther 1997;281:624–8.
61. Preis M, Korc M. Signaling pathways in pancreatic cancer. Crit Rev Eukaryotic Gene Expr 2011;21:115–29.
62. Freeman JW, DeArmond D, Lake M, Huang W, Venkatasubbarao K, Zhao S. Alterations of cell signaling pathways in pancreatic cancer. Front Biosci 2004;9:1889–98.
63. Altomare DA, Testa JR. Perturbations of the AKT signaling pathway in human cancer. Oncogene 2005;24:7455–64.
64. Gullino PM, Grantham FH. Studies on the exchange of fluids between host and tumor. III. Regulation of blood flow in hepatomas and other rat tumors. J Natl Cancer Inst 1962;28:211–29.
65. Guo X, Ma N, Wang J, Song J, Bu X, Cheng Y, et al. Increased p38-MAPK is responsible for chemotherapy resistance in human gastric cancer cells. BMC Cancer 2008;8:375.
66. Zheng X, Carstens JL, Kim J, Scheible M, Kaye J, Sugimoto H, et al. Epithelial-to-mesenchymal transition is dispensable for metastasis but induces chemoresistance in pancreatic cancer. Nature 2015;527:525–30.
67. White PB, Ziegler KM, Swartz-Basile DA, Wang SS, Lillemoe KD, Pitt HA, et al. Obesity, but not high-fat diet, promotes murine pancreatic cancer growth. J Gastrointest Surg 2012;16:1680–5.
68. Tam J, Duda DG, Perentes JY, Quadri RS, Fukumura D, Jain RK. Blockade of VEGFR2 and not VEGFR1 can limit diet-induced fat tissue expansion: role of local versus bone marrow-derived endothelial cells. PloS One 2009;4:e4974.

Published OnlineFirst May 31, 2016; DOI: 10.1158/2159-8290.CD-15-1177

69. Fukumura D, Ushiyama A, Duda DG, Xu L, Tam J, Krishna V, et al. Paracrine regulation of angiogenesis and adipocyte differentiation during in vivo adipogenesis. Circ Res 2003;93:e88–97.
70. Surwit RS, Feinglos MN, Rodin J, Sutherland A, Petro AE, Opara EC, et al. Differential effects of fat and sucrose on the development of obesity and diabetes in C57BL/6J and A/J mice. Metabolism 1995;44:645–51.
71. Bardeesy N, Aguirre AJ, Chu GC, Cheng KH, Lopez LV, Hezel AF, et al. Both p16(Ink4a) and the p19(Arf)-p53 pathway constrain progression of pancreatic adenocarcinoma in the mouse. Proc Natl Acad Sci U S A 2006;103:5947–52.
72. Wang Y, Zhang Y, Yang J, Ni X, Liu S, Li Z, et al. Genomic sequencing of key genes in mouse pancreatic cancer cells. Curr Mol Med 2012;12:331–41.
73. Diop-Frimpong B, Chauhan VP, Krane S, Boucher Y, Jain RK. Losartan inhibits collagen I synthesis and improves the distribution and efficacy of nanotherapeutics in tumors. Proc Natl Acad Sci U S A 2011;108:2909–14.

Published OnlineFirst May 31, 2016; DOI: 10.1158/2159-8290.CD-15-1177

AACR American Association for Cancer Research

CANCER DISCOVERY

Obesity-Induced Inflammation and Desmoplasia Promote Pancreatic Cancer Progression and Resistance to Chemotherapy

Joao Incio, Hao Liu, Priya Suboj, et al.

Cancer Discov 2016;6:852-869. Published OnlineFirst May 31, 2016.